ANALYSIS OF VARIATION OF TOTAL ELECTRON CONTENT (TEC) OVER TWO EQUATORIAL LOCATIONS IN NIGERIA

BY

MUHAMMAD USMAN SHEHU
SPS/12/MPY/00026

BEING AN M.Sc. DISSERTATION SUBMITTED TO THE DEPARTMENT OF PHYSICS BAYERO UNIVERSITY KANO, IN PARTIAL FULFILMENT OF THE REQUIREMENT FOR THE AWARD OF MASTER OF SCIENCE DEGREE IN PHYSICS

SEPTEMBER, 2016

DECLARATION

I hereby declared that this work (ANALYSIS OF VARIATION OF TOTAL ELECTRON CONTENT IN TWO EQUATORIAL STATIONS) is the product of my own research effort; undertaken under the supervision of (Dr RABI'A SALIHU SA'ID) and has not been presented and will not be presented elsewhere for the award of a degree or certificate. All sources have been duly acknowledged.

Sign/ date.....

Muhammad Usman Shehu

SPS/12/MPY/OOO26

CERTIFICATION

This is to certify that the research work for this thesis and the subsequent preparation of this thesis by (Muhammad Usman Shehu SPS/12/MPY/00026) were carried out under my supervision

Dr Rabi'a Salihu Sa'i

…… ……

Supervisor Sign **Date**

Dr T.H Darma

……. …….

Head of Department Sign **Date**

APPROVAL PAGE

This thesis work has been carefully examined and approved after satisfying the requirement for the award of degree of MASTER OF SCIENCE IN PHYSICS

…….. **……**

External Examiner **Sign and Date**

……. **……..**

Internal Examiner **Sign and Date**

……. **…….**

SUPERVISOR **Sign and Date**

…… **……**

HEAD OF DEPARTMENT **Sign and Date**

ACKNOWLEDMENT

My profound gratitude goes to Almighty ALLAH the creator and the sustainer of creations for his numerous blessing on me throughout my life as a whole .My appreciation goes to my parents, for their support, care provision and advice May ALLAH reward them all with Aljannatul firdaus Ameen.

I am grateful to my supervisor Dr R S Said, I am indebted to you mom for all your encouraging advise, professional guide and motherly support May Allah reward you and your family with his wonderful blessing amen, It has been my great fortune to be able to work in my thesis efforts with such competent individual

May all those who have contributed either directly or indirectly, expressly or impliedly or even by implications towards the success of my academic pursuit be well rewarded. I feel highly honored and passionately grateful indeed.

Finally, I wish to recognize and appreciate my brothers for all they have contributed so unselfishly. In particular, I wish to thank Yusuf Abdullahi, Ibrahim Shehu, Nuradeen Shehu, Dayyabu Shehu, Surajo Shehu and Nasiru Shehu I wish also to recognize my indebtedness to

Mal Yahaya Yusuf, I shall not forget his encouragement, advice and support during my early years of graduate and post graduate study.

Several other persons deserve recognition for their support of this project. Foremost is Dr B .I Tijjani, Dr M .H. Ali Dr Fatima S Koki and all other lecturers in Physics Department for their kind contribution, advice and encouragement may ALLAH bestow his mercy on you amen.

DEDICATION

This thesis is dedicated to Almighty Allah and to my mother Hajiya Aishatu Usman and to my Father Late Alhaji Shehu Usman Abdullahi

TABLE OF CONTENTS

CHAPTER ONE

CHAPTER TWO

CHAPTER THREE

CHAPTER FOUR

CHAPTER FIVE

ABSTRACT

In this work, the Total Electron Content (TEC) of the ionosphere is derived by analyzing dual frequency signals from the Global Positioning System (GPS) recorded from two stations (Birnin Kebbi and Zaria) in Nigeria during the year 2012 (Rz = 57.37). The mean diurnal, monthly and seasonal variation of equatorial ionosphere for these stations is studied. The highest TEC values were found to have occurred from 13h00 to 17h00, local time (LT), throughout the year. The lowest values have been observed in summer with the highest values of 55 TECU being exhibited during equinoctial months. The observed GPS-TEC has been compared with the TEC derived from the IRI model-2012. The models followed the diurnal, monthly and seasonal variation shapes of the observed values of TEC, however the IRI–TEC under estimated the derived TEC in all the months and seasons for this study. The data was subjected to RMSE analysis to find out the performance of the model compared to the observed data. It was found that the seasonal variation in the IRI model performed better in June solstice and underestimated during all the Months and seasons.

CHAPTER ONE

1.0 INTRODUCTION

The history of ionospheric research start with the first transatlantic radio operated by Guglielmo Marconi in 1901. The distance between the transmitter and the receiver was about 3500 km. adopting a straight line propagation, this wireless experiment would not be attained because of the sphericity of the earth. Explanation of the physical phenomenon involved in the transatlantic transmission emerged from Arthur Kennelly and Oliver Heaviside, who were the first to predict the existence of a reflective atmospheric layer. This region, called E-layer, consists of an ionized gas layer located at an altitude of about 100–150 km and has been foremost observed by Edward Appleton in 1924. E-layer ionization rate and altitude are varying with local time and latitude, which implies that radio wave propagation is changing over time, as observed by Marconi in another experiment. Considering this particular behavior with respect to incident radio waves, the following definition of the ionosphere has been proposed by Davies (1990): "The ionosphere is defined as that part of the upper atmosphere where sufficient ionization can exist to affect the propagation of radio waves". With the first artificial satellites came the discovery and the study of the ionospheric structure and its strong relationships with geomagnetic and solar environments. Later, the development of navigation systems like the American Global Positioning System (GPS) opened new perspectives in ionospheric study as they offer a global coverage at any time (Wautelet. 2013). More particularly, the ionosphere remains the main error source in satellite positioning so that the understanding of its spatial and temporal behaviors will play a key role in precise positioning techniques.

1.1 SOLAR ATMOSPHERE AND SPACE WEATHER

Without the Sun, planetary ionosphere would not exist. Indeed, production of free electrons in the ionosphere mainly results from interactions between neutral molecules and Extreme Ultraviolet (EUV) or X-rays coming from the external regions of the Sun. Ionization rate is

strongly related to the incoming radiation, which results in regular cycles in the electron concentration N_e. Superimposed to the ionospheric regular behavior are the so-called irregularities, whose a given part find their origin in large-scale solar phenomena such as coronal eruptions propagating into the interplanetary medium.

1.2 THE IONOSPHERE

The ionosphere is a region of the upper atmosphere, from about 85km to 600km altitude, and includes the thermosphere and part of the mesosphere and exosphere. The ionosphere is the ionized component of the atmosphere and most of the ionosphere is electrically neutral, but when solar radiation strikes the chemical constituent of the atmosphere free electrons and positive ions are produced generally in equal number (Fayose, *2012;* Kelly, 1989).This occurs on the Sunlit side of the earth and only the shorter wavelengths of solar radiation (X-ray) are energetic enough to produce this ionization. The presence of these charged particles makes the upper atmosphere an electrical conductor. There is still a great deal to understand about the physical and chemical processes controlling the behavior of ionosphere, particularly with respect to its dynamic response to solar influences. Characterizing the ionosphere is of utmost interest due to its effect on modern technologies (Rabi'u, 2011) such as civilian and military communication, navigation systems and surveillance, etc. For many communication and navigation systems, this arises because the systems use signal transmitted to and from satellite which must therefore pass through the ionosphere (Klobuchar, 1996). For effects imposed by ionosphere on communication and navigation, it is therefore necessary to correct the signals. To do that the properties of ionosphere such as its variability with respect to magnetospheric disturbance, time of the day, season of the year and solar cycle variability must be well understood (Darose *et al.,* 1973). For more than 70 years scientist around the globe have been observing ionospheric variability using different observing technique e.g. geostationary satellite beacon signals (Huang, 1978).

1.3 SCIENTIFIC RESEARCH ON IONOSPHERIC PROPAGATION

Scientists also are exploring the structure of the ionosphere by a wide variety of methods, including passive observations of optical and radio emissions generated in the ionosphere, bouncing radio waves of different frequencies from it, incoherent scatter radars such as the EISCAT, Sondre Stromfjord, Millstone Hill, Arecibo, and Jicamarca radars, coherent scatter radars such as the Super Dual Auroral Radar Network (SuperDARN) radars, and using special receivers to detect how the reflected waves have changed from the transmitted waves.

A variety of experiments, such as HAARP (High Frequency Active Auroral Research Program), involve high power radio transmitters to modify the properties of the ionosphere. These investigations focus on studying the properties and behavior of ionospheric plasma, with particular emphasis on being able to understand and use it to enhance communications and surveillance systems for both civilian and military purposes. HAARP was started in 1993 as a proposed twenty year experiment, and is currently active near Gakona, Alaska.

The SuperDARN radar project researches the high- and mid-latitudes using coherent backscatter of radio waves in the 8 to 20 MHz range. Coherent backscatter is similar to Bragg scattering in crystals and involves the constructive interference of scattering from ionospheric density irregularities. The project involves more than 11 different countries and multiple radars in both hemispheres. Scientists are also examining the ionosphere by the changes to radio waves, from satellites and stars, passing through it.

1.4 IONOSPHERIC LAYERS

The ionosphere has historically been divided into regions (D, E, and F), with the term “layer “referring to the ionization within a region according to the electron density as shown in fig 1.1. These layers are named D (50-90 km), E (90-140 km), F1 (140-210 km), and F2 (210-1,000 km), respectively, with F2 usually being the layer of maximum electron density. The altitude and thickness of those layers vary with time, as a result of the changes in the sun’s

radiation and the Earth's magnetic field. The early detected was the E layer, at night the F layer is the only layer of significant ionization present, while the ionization in the D and E layers become much more heavily ionized, as does the F layer, which develops an additional, weaker region of ionization known as the F1 layer the F1 layer disappears during the night and is more pronounced in the summer than in the winter .The F2 persist by day and night and is the region mainly responsible for the refraction of radio waves. D layer ionization is a function of the solar flow. The ions are formed by the ionization of atmospheric neutrals by X-ray radiation and solar Lyman α radiation. This region vanishes at night due to the combination of the ions and electrons. HF radio waves are not reflected by this region, the main impact of which is absorption of high-frequency radio waves. Similarly to the D layer, the E layer shows a diurnal behavior with a maximum ionization at local noon. In this region, ions consist primarily of O_2 produced by the absorption of solar radiation, and NO^+ formed by charge transfer collisions with other ions ionized by coronal X-rays. In auroral region, solar particle precipitation can produce radio scintillation effects in the E layer. F layer which is the last layer of ionosphere with a height of 120 to 800 km; Pressure: 10^{-4}pa; Temp.: 1000° C; the electron concentration is up to 10^{11} e^-/m^2: This layer is formed by ionization of atomic oxygen by Lyman emissions and emissions from He. This region is sometimes divided into F1 and F2 sub-layers. The maximum electron concentration of the F1 region is close to 200km. This layer, in which O^+ ions transfer charge to neutrals to form NO^+, disappears at night due to dissociative recombination. The peak of the F2layer electron concentration is approximately at 350km. The degree of ionization in the ionosphere depends essentially on the Sun, amount of radiation received from the Sun. Hence, there is a diurnal effect as the solar radiation received locally varies during the day. There is a seasonal effect, since the local winter hemisphere is tipped away from the Sun, thus receiving less solar radiation. Different geographic regions of the Earth's surface (polar, auroral zones, mid-latitudes and equatorial regions) are also not equal

with respect to the solar radiation they receive (Rob, 2014) Recent researches show that earthquakes can affect the ionosphere by the propagation through the atmosphere of gravitational waves. As in the worked of Tsugawa *et al*. (2011) firstly reported the detailed ionospheric disturbances following the 2011 Tohoku-Oki earthquake on the basis of the high resolution GPS total electron content observation in Japan. By using dense GPS data in Japan, Rolland *et al*. (2011) analyzed the ionosphere response and found three different types of waves in the TEC signal over Japan. Liu *et al.* (2011b) studied seismo-traveling ionospheric disturbances triggered by seismic and tsunami waves of the Tohoku-Oki earthquake. Furthermore, similar pre-seismic TEC anomalies were seen in other great earthquakes including the 2010 Chile earthquake (M8.8), the 2004 Sumatra–Andaman (M9.2) le., *et al*. 2013) studied the ionospheric anomalies prior to the M9.0 Tohoku-Oki earthquake using the GPS TEC derived from jet propulsion laboratory, it was found that TEC show some significant enhancements occurred on March 8, 3 days before the great Tohoku-Oki earthquake. He further suggest that, the variation of $F_{10.7}$ (solar emission) index also shows large increase in solar radiation in the same period. The extreme enhancement persistently located around the adjacent region of epicenter and the magnetic conjugate point for as long as 16 h, which indicate that these anomalies might be related to the March 11, 2011 Tohoku-Oki earthquake. In addition, a geomagnetic disturbance with Kp = 4 occurred on March 7. These anomalies may also be contributed partly by the geomagnetic disturbance.

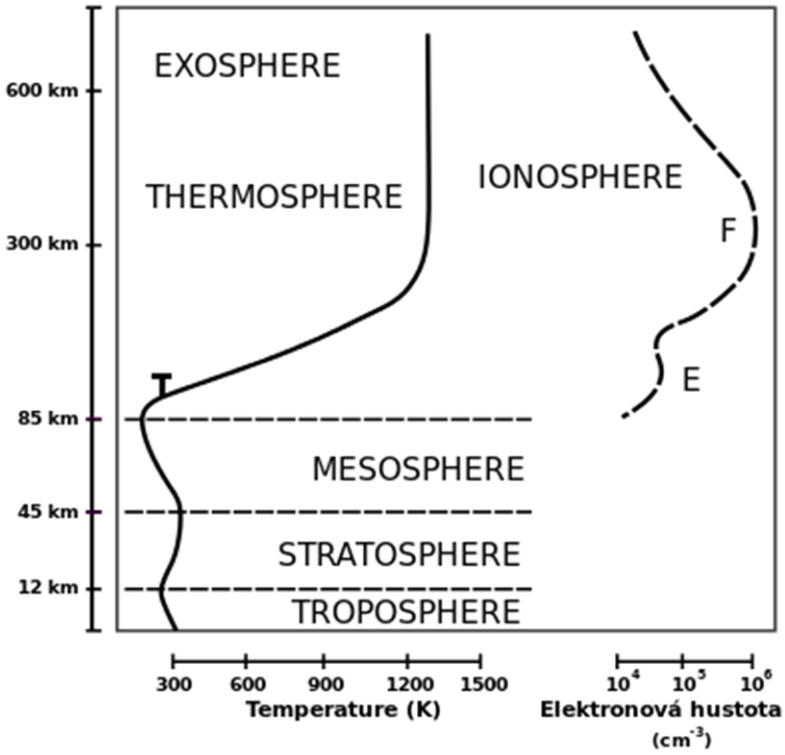

Fig 1.1. Various layers of the ionosphere and their respective heights above ground. The density in the ionosphere varies considerably, as shown.

1.5 IONOSPHERIC IRREGULARITIES

This is the fluctuation of the ionospheric parameters in the ionosphere. It can be detected by their ability to scatter radio waves. Irregularities below 10MHz can cause spread F and plasma bubbles which can disrupt radio communication and leads to scintillation. Above 10MHz, it is useful in amateur radio propagation. Each layer in the ionosphere has its own irregularities. Studies have shown that ionospheric irregularities show dependence on season. Post-midnight equatorial F-region irregularities are known to develop mainly during sosticial months.

1.5.1 High Latitude

Irregularities are always accompanied by bursts of small scale field-aligned currents. High latitude electron density irregularities occur as frequently as plasma bubbles at low latitude. It also depends on magnetic variation. It has been observed that irregularities occur during geomagnetic stormy periods. It is mainly controlled by perturbation of the zonal electric field

i.e. prompt penetration of eastward electric fields (PPEFs) and disturbance dynamo electric fields (DDEFs) (Maruyama *et al.*, 2004). At solar maximum, occurrence rate of post-midnight equatorial F-region irregularities (EFI) is high in African and Pacific region, moderate in the South-east Asian region and low in the Peruvian region.

1.5.2 Spread F

It is a general term used to denote existence of ionospheric irregularities in the RF (Range type spread F) measurement data. It is also called equatorial irregularities and it occurs along the F-layer. Equatorial spread F is mainly night-time events as they occur in the evening hours between 2100LT and 0100LT during equinoxes. They seem to be associated with the rising plumes of ionization due to the evening rise of the fountain effect. The basic mechanism of the generation and development of low latitude spread F is the gravitational Rayleigh-Taylor instability and the instability of ExB. Rayleigh Taylor instability is instability of an interface between two fluids of different densities which occurs when the lighter fluid is pushing the heavier fluid. During geomagnetic storm, the low latitude spread F is mainly controlled by the perturbations of the zonal electric field at equator (Chakraborty and Hajra, 2010). Under quiet condition, the June solstice is a low-occurrence season of range-type spread F, topside PBs and GPS amplitude scintillations. Spreading of F-region traces on ionogram has been divided into two:

1. Range spreading (at lower latitudes)
2. Frequency spreading (at higher latitudes)

For seasonal variation, range-type spread F (RSF) occurrence has maximum values in March and September while frequency-type spread F (FSF) occurrence peaks at June. For night-time variation, RSF peak at 2300LT and FSF peaks at 0300LT.

1.5.3 Plasma Bubbles

It refers to irregular plasma density depletions observed by satellite and radar backscatter in the topside ionosphere that is generated on the bottom-side of night-time equatorial F-region and rises to higher altitude. It is used to describe a night-time equatorial ionosphere within which the plasma density is significantly reduced (Sharma *et al*, 2012). It can be identified by observing ion density perturbations and enhanced upward ion drift velocity (driven by polarization electric field). They are usually formed or grow in the evening sector and slowly decay after midnight in E-region. Series of PBs are generated through the non-linear Rayleigh-Taylor instability process over a large longitudinal range. Plasma bubble-associated irregularities often profoundly impact satellite communication and navigation systems and produce scintillations. It was suggested that the equatorial electro jet (EEJ) is a useful parameter for predicting the PBs development.

1.6 IONOSPHERIC SCINTILLATIONS

There are certain regions of the ionosphere (mainly the high latitude and low latitude F-region,) and certain local times (principally after sunset) when the ionosphere may become highly turbulent. "Turbulence" is defined here as the presence of small-scale (from centimeters to meters) structures or irregularities imbedded in the large-scale (tens of kilometers) ambient ionosphere. Under favorable conditions, plasma density irregularities are generated just after sunset in the equatorial region and may last for several hours. At high latitudes, these irregularities may be generated during either the daytime or at night. For both low and high latitude regions these small-scale irregularities occur most frequently during the solar cycle maximum period .The existence of these small-scale structures can seriously affect the nature of radio waves as they propagate through the ionosphere where they are imbedded. The bigger the amplitude fluctuations of the scintillated signal the greater the impact on Communication and Navigation system

1.7 .TECHNIQUES FOR PROBING THE IONOSPHERE

- Radio propagation -up to satellite altitudes
- Geomagnetic field studies -altitude > 90 km

- Rocket -up to ionospheric altitudes
- Satellites -up to satellite altitudes
- Radar -up to satellite altitudes
- Lidar-up to satellite altitudes(Rabiu ;2011)

1.8. AIM OF THE RESEARCH

The main aim of this research is to use the data as measured by GPS to find the diurnal monthly and seasonal variation and device ways by which understanding of the variation in total electron content can help in reducing the errors caused by ionospheric variability.

1.9. OBJECTIVES

- Obtain the TEC data from the two GPS stations
- Analyse TEC Variability and validation of IRI model 2012
- To generate geo reference network for various applications
- Contribute data for the adequate correction for the effect of ionospheric propagation

1.10. STATEMENT OF THE PROBLEM

- Various effects as a result of the ionospheric dynamics impact on communication and navigation. It is therefore necessary to correct the signals to the desired usage. To do this the properties of ionosphere such as its variability with respect to magnetospheric disturbance, time of the day, season of the year and solar cycle variability must be well understood.

1.10. SCOPE AND LIMITATIONS

- The research is intended to cover two areas within Nigeria; Zaria and Kebbi States. These are locations in northern Nigeria, where GPS are installed.

- The research will only make use of data from these two stations: Ahmadu Bello University, Zaria and Kebbi State GPS station at Birnin Kebbi.

CHAPTER TWO

LITERATURE REVIEW

2.1 INTRODUCTION

The ionosphere is a highly variable and complex physical system, where ions and electrons are present in quantities sufficient enough to affect the propagation of radio waves (Matsushita and Wallace, 1967). Ionospheric behavior has been widely studied using different observing techniques such as the ionosonde measurements, trans-ionospheric radio signals and incoherent radar system (Whitten and Poppoff, 1971). In the last decade, Global Positioning System (GPS) data have been used extensively for the study of the ionosphere (Chauhan and Singh, 2010; da Costa *et al.*, 2004; Ezquer *et al*., 2004; Rama Rao *et al.* 2006).

The phase approach and Doppler shift of a carrier, group retardation and time delay of a modulation, Faraday rotation of the polarization and wedge refraction of the wave direction are all dependent in some way on the line integral of the electron density along the ray path through the ionized atmosphere, the so called total electron content (Darvies, 1990). Total electron content is a key parameter in the moderation of ionospheric effects on radio systems (Parkinson, 1990). In numerous applications involving radio links between satellites and ground, which play vital roles in the modern technology of communications, navigation and surveillance, the propagation departs from free space conditions in various ways with significant effects for the reliability and accuracy of the service. The ability to make adjustment for the effects on the propagation of the electron content and its temporal and spatial variations (Davies, 1980; Kumar and Singh, 2009) thus becomes an essential component in the reliable operation of the system. Indeed, adequate correction for the effect of ionospheric propagation may represent a limiting error for the accuracy of some uses of the technology (Kersley, 2002). Total electron content has been measured experimentally since the 1960s using a variety of

different techniques. Some early measurements involved determination of the polarization rotation of VHF transmissions from the first-generation of geosynchronous communications satellite (Titheridge, 1996; Gariot *et al*., 1967; Walker and Ting, 1972; Soicher and Gorman, 1985). Later it became possible to exploit the signals from the various satellite navigation and positioning systems, like NNSS (Navy Navigation Satellite System) and more recently GPS(Chin-Chun Wu *et al*., 2003; Alothman *et al*., 2011; Shimeis *et al*. 2012). A vast body of data and information about total electron content has been amassed over the years from numerous locations giving almost worldwide coverage. In addition, products have been developed in the form of regional and global models yielding total electron content, while more recently maps are now routinely available of the parameter on the Internet. Another recent advance has been the application of tomographic techniques to invert electron content measurements to obtain images of ionospheric electron density. (Kersley, 2004)

2.2. IONOSPHERIC VARIABILITY

The ionosphere varies greatly because of changes in the two sources of ionization and because it responds to changes in the neutral part of the upper atmosphere in which it is embedded. This region of the atmosphere is known as the thermosphere. Since it responds to solar EUV radiation, the ionosphere varies over the 24-hour period between daytime and nighttime and over the 11-year cycle of solar activity. The other main source of variability in the ionosphere comes from charged particles responding to the neutral atmosphere in the thermosphere. The ionosphere responds to the thermospheric winds; they can push the ionosphere along the inclined magnetic field lines to a different altitude. The ionosphere also responds to the composition of the thermosphere, which affects the rate that ions and electrons recombine. During a geomagnetic storm, the energy input at high latitudes produces waves and changes in thermospheric winds and composition. This produces both increases (“positive phases”) and decreases (“negative phases”) in the electron concentration. The changes experienced by a

radio signal when it propagates through the ionosphere depend on the carrier frequency and electron density of the ionosphere, the ratio between the group propagation velocity (v) and the speed of light in vacuum c. This can be described as refractive index and is given by

$$n_{ion} = \frac{c}{V_{gr}} \qquad (2.1)$$

The refractive index of the ionosphere n_{ion} can affect radio GPS signals as they pass from satellite to the ground in a number of ways (Rama Rao, 2006). One of the significant effects is that the GPS signals traversing the ionosphere undergoes an additional delay proportional to the total number of electron content in the cross section volume measured in TEC unit. The dual frequency receiver uses two frequencies L_1 and L_2 to compensate for that ionospheric delay which remove this effect at least to a first order approximation where the refractive index is a function of frequency. The ionospheric time delay at the L1 carrier frequency of f_1 as given by (Klobuchar, 1996).

$$t_1 = 40.3\left(\frac{TEC}{Cf_1^2}\right) \qquad (2.2)$$

where C is the speed of light in free space the single-frequency band (L1) which was then an important parameter for estimating TEC has been further augmented to dual-frequency bands (L1) and (L2) by the US DoD. One of the advantage of the dual-frequency usage over a single-frequency receiver is that it operates on the 1.57542 GHz (L1) and 1.22760 GHz (L2) frequencies simultaneously. This operation permits measurement of the relative phase delay between the two signals, defined as the slant TEC, or the total number of electrons in a column of cross-sectional area of $1m^2$ along the signal path between the satellite and the receiver. A dual frequency (f_1 and f_2) receiver measures the difference in time delay between the two frequencies, $\Delta t = t_2 - t_1$, given by

$$\Delta \boldsymbol{t} = \mathbf{40.3}\left(\frac{\boldsymbol{TEC}}{\left[\left(\frac{\mathbf{1}}{\boldsymbol{f_2^2}}\right)-\left(\frac{\mathbf{1}}{\boldsymbol{f_1^2}}\right)\right]}\right) \qquad \textbf{(2.3)}$$

Thus, the time delay (Δt) measured between the L_1 and L_2 frequencies is used to calculate the TEC along the ray path. Group refractive index then leads to

$$n_{ion} = 1 + \frac{40.3N_e}{f^2} \qquad (2.4)$$

Where N_e = number density of electrons and f is the signal carrier frequency. If we write the ionospheric propagation time as integration of propagation speed over the propagation path and include equation (2.4)

$$T = \int_s \frac{1}{v_{ion}} ds = \int_s \frac{n_{ion}}{C} ds \qquad (2.5)$$

Ionospheric propagation delay can be converted to the equivalent distance (Δρ) by multiplication with the speed of electromagnetic wave in vacuum: thus $\Delta\rho = c\Delta t$

$$\Delta\rho_{ion} = \frac{40.3}{f^2}\int_s N_e ds \qquad (2.6)$$

Ionospheric group delay can then be written (Najman and Kos, 2014) as

$$\Delta t_{gr} = \frac{40.3TEC}{f^2} \qquad (2.7)$$

And the Total Electron Content (TEC) is obtained by integrating the product of the total number of electrons and the distance as shown in equation (2.8).

2.3.SOLAR CYCLE AND ROTATION

The Sun follows an activity cycle, called *solar cycle*, driven by the solar dynamo and whose period and amplitude are varying from a cycle to another. On average, a solar cycle lasts 11 years and its maximum level is reached after a rapid increase of 4 years. Monitoring of the

solar cycle is mainly achieved by the analysis of several quantities called indices. Among them is the *International Sunspot Number,* which measures the number of sunspots and groups of sunspots observed on the photosphere.

Another solar activity proxy is $F_{10.7}$, the radio flux at wavelength 10.7 cm (2.8 GHz), observed daily at the radio station of Penticton, Ottawa (Canada) since 1950. This index is quite well correlated with the sunspot number although the observed layer on the Sun is not identical (photosphere for sunspots and top of the chromosphere for *F*10*:*7). Scientific literature proposes lots of other solar activity indices such as the Total Solar Irradiance (TSI) (De toma, 2001).

2.3.1 **Core-To-Wing Index**.

The Sun also accomplishes a rotation on itself whose period is approximately 25 days at the solar equator and up to 35 days at the poles, called *differential rotation*. From the Earth's point of view, the mean solar rotation, called *synodic rotation period*, lasts 27.3 days (wautelete, 2013). Solar corona extends up to the limit of the interstellar space. As the Sun is rotating on its axis, solar wind and IMF do not travel the interplanetary medium radially but follow a spiral shape which crosses the Earth's orbit with an angle of 45^0

2.4 SOLAR ACTIVITY

2.4.1. Corotating Interaction Regions

During solar minimum, solar magnetic field is globally bipolar with high-latitude coronal holes blowing a fast solar wind while the equatorial region bubbles out a slow solar wind, originating from bright coronal loops. When a fast wind region catches up with a slow one, a front shock appears and the resulting region is called a Corotating Interaction Region (CIR). CIRs are recurrent patterns in the heliosphere since they are associated with solar rotation. Their occurrence can be foreseen by monitoring IMF and solar wind parameters.

2.4.2 EUV and X- Rays' Variability

The solar emission in EUV and X-Ray domains is subject to an extremely large variability over the solar cycle. As those radiations are responsible for the ionization of the Earth's ionosphere identifying the phenomena responsible for their enhancements and depletions can therefore help to understand ionospheric variations. The intensity of EUV and X radiations is strongly correlated with the solar cycle: during solar maximum, Sun's photosphere is peppered with sunspots from which large coronal loops are emerging. Bright emission in the EUV/X lines is therefore enhanced during high solar activity periods. In addition to this modulated background, transient events called *solar flares* release tremendous amount of energy in the form of EUV and X rays. Those radiation bursts, due to magnetic reconnection between coronal loops, are responsible for sharp ionization increases in the illuminated ionosphere.

2.5. GENERAL FEATURES OF THE IONOSPHERE

Ionospheric composition and morphology is varying with the time of the day, season, solar activity and geomagnetic conditions. According to geomagnetic dip angle, one can subdivide the ionosphere into three principal regions, each of them exhibiting specific features and mechanisms which are Equatorial, aurora and mid latitude region

2.5.1 Equatorial Ionosphere

Due to the unique geometry of the magnetic field at the equator and low latitudes, the ionospheric effects on GPS signals are more pronounced in the low latitudes than in the other latitudes .The equatorial and low latitude ionosphere is characterized in terms of latitudinal ionization by a trough at the magnetic equator and crests at about $\pm 17^0$ magnetic latitude, a feature referred to as the equatorial ionization anomaly (EIA) The cause of the anomaly is often attributed to the so-called "fountain effect it is the eastward electric field at the equator that gives rise to an upward $E \times B$ drift during the daytime figure 2 and 3. After the plasma is lifted to greater heights it is able to diffuse downward along magnetic field lines under the

influence of gravity and pressure gradient forces. The daytime dynamo generated eastward electric field combined with the northward geomagnetic field lifts the equatorial ionosphere to 700 km to over one thousand kilometers (Rabiu, 2011). After losing momentum, the electrons diffuse along the field lines to either side of the equator to form two crests in response to the diurnal variations of the dynamo electric field (Abdullahi *et al.*, 2012). the anomaly crest begins to form around; 09:00 LT on a normal day and increases with a constant speed .This speed is maintained till shortly before noon when the pole ward motion is slowed and reversed at around 14:00 LT During this time, the anomaly crest is most intense, showing the characteristic tilt, an approximate alignment of its core along the geomagnetic field lines and the asymmetric behavior. Thereafter, the crest weakens and recedes slowly toward the equator. The ionosphere in Nigeria is unique because of her location near and at the equator, where a lot of phenomena such as the equatorial anomaly and fountain effect make it good for studies. Rabiu *et al.* (2014) reported on the analysis of TEC using GPS near and on magnetic equator while Bolaji *et al.* (2012) reported on the variability of TEC over an African station during a low solar activity. Bolaji *et al*. (2013) also reported on Global Positioning System (GPS) receiver and the Magnetic Data Acquisition System (MAGDAS) magnetometers, which are co-located at the University of Ilorin (Geographiclatitude:8.471^{0}N, GeographicLongitude:4.681^{0}E, Geo- magneticLatitude:1.821^{0}S), Nigeria. Bolaji has shown that late reversal of nighttime westward electric field to eastward electric field during pre-sunrise to sunrise hours could inhibits generation of EIA during the rising flank which reveals that when the EIA is suppressed, photo-ionization dominates, and no pre-noon peaks can be formed on DTEC variability. Otherwise, photo-ionization is suppressed and pre-noon peaks are formed on DTEC variability. Also, when there is a slight developed EIA, there is competition between EIA and photo-ionization, the expected pre-noon peak on DTEC variability were found delayed and will be formed during the noon period or later depending

on the present neutral wind. The seasonal and geomagnetic effects on the equatorial ionospheric anomaly crest by analyzing TEC data acquired from a chain of nine ground GPS stations at and in the neighborhood of Taiwan during the solar minimum period between September 1996 and August 1997, was studied by Wu *et al.* (2004). They found that the surveyed data indicates semiannual variation in TEC at anomaly, with maxima at equinoxes. They further demonstrated that the monthly EIA was well correlated with Dst (Disturbance Storm Time) and weakly correlated with F10.7. Kumar and singh, (2009) studied variation of daily EIA crest in TEC observed at Varanasi during the solar minimum period of May 2007 to April 2008 using GPS Data. The daily EIA crest in TEC shows both the seasonal and semiannual variation, which shows maxima in equinox (October and April) months and minimum in winter (December) and summer (July).

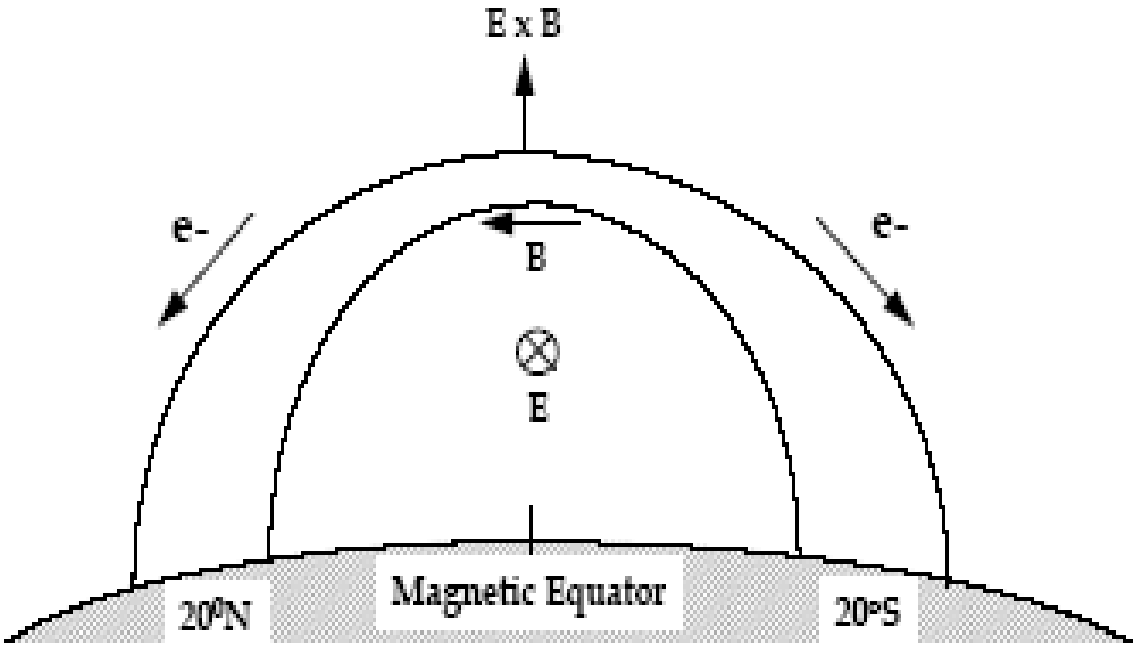

FIG 2.1 Magnetic Trough (Source:Rabiu 2011)

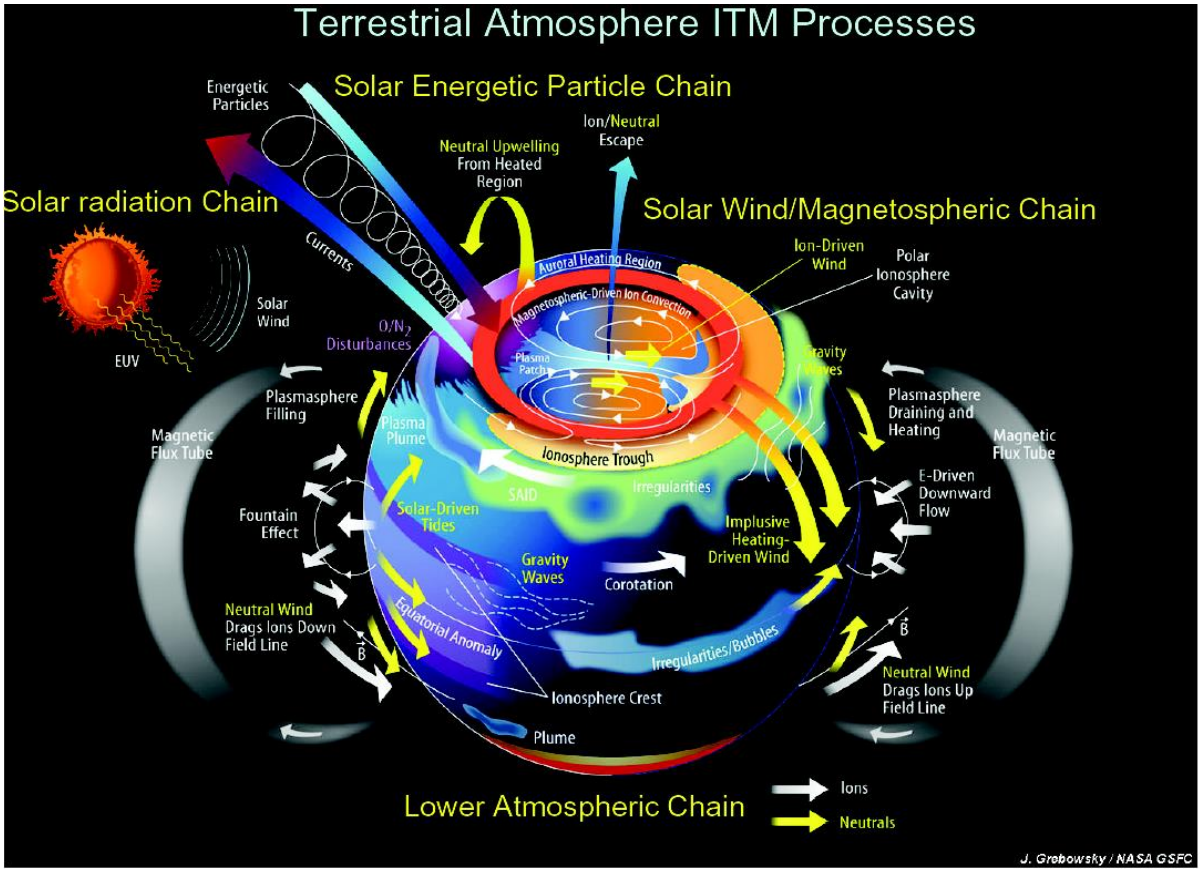

FIG .2.2 Terestrial Atmosphere (Source: Rabiu 2011)

2.5.2. Polar (or auroral) Regions.

Also called high-latitude regions, the auroral regions are located above the 60° parallels, where the nearly vertical magnetic field lines allow the ionosphere to be in close relationship with the magnetosphere. Magnetospheric conditions are mainly driven by space weather phenomena, in particular by the solar wind carrying the IMF. This implies energetic particles like protons and electrons to precipitate directly in the polar ionosphere, leading to highly variable electron density and TEC. While the ionization in equatorial and mid-latitude regions is mainly due to solar radiations, ionization in Polar Regions is also partially due to particle precipitation, hence a strong geomagnetic control of these regions. This is particularly true during the polar night (absence of EUV solar flux).

2.5.3. Mid-Latitude Regions.

These regions extending from about 20 to 60°, electron density results from the equilibrium between ionization and losses, but also from transport processes like those due to neutral winds or ambipolar diffusion. Here, the ionosphere is neither under the influence of the fountain effect nor affected by polar particle precipitation. However, if one could expect larger $f0F2$ and VTEC values during summertime (due to a higher ionization level), observations show the opposite, exhibiting *Ne* and VTEC maximum in winter. This is the so-called *winter anomaly* is due to changes in the molecular-to-atomic ratio of the neutral atmosphere, which implies a variation in the recombination rate. This ratio exhibits larger values during summer than during winter; electron recombination is therefore more efficient in the summer hemisphere, hence a lower electron density.

2.6. GPS

The Global Positioning System (GPS) is a satellite-based navigation system that was developed by the U.S. Department of Defense (DoD) in the early 1970s. Initially, GPS was developed as a military system to fulfill U.S. military needs. However, it was later made available to civilians, and is now a dual-use system that can be accessed by both military and civilian users. GPS provides continuous positioning and timing information, anywhere in the world under any weather conditions. Because it serves an unlimited number of users as well as being used for security reasons, GPS is a one-way-ranging (passive) system (Langley, 1990). That is, users can only receive the satellite signals (Elrabbany, 2002).

2.7. HOW WOULD THE IONOSPHERE AFFECT GPS MEASUREMENT?

The ionosphere is a dispersive medium, which means it bends the GPS radio signal and changes its speed as it passes through the various ionospheric layers to reach a GPS receiver. Bending the GPS signal path causes a negligible range error, particularly if the satellite elevation angle is greater than 5^0. It is the change in the propagation speed that causes a significant range error,

and therefore should be accounted for. The ionosphere speeds up the propagation of the carrier phase beyond the speed of light, while it slows down the PRN code (and the navigation message) by the same amount. That is, the receiver-satellite distance will be too short if measured by the carrier phase and too long if measured by the code, and compared with the actual distance (Hoffmann; *et al*. 1994). The ionospheric delay is proportional to the number of free electrons along the GPS signal path, called the total electron content (TEC). TEC, however, depends on a number of factors: (1) the time of day (electron density level reaches a daily maximum in early afternoon and a minimum around midnight at local time); (2) the time of year (electron density levels are higher in winter than in summer); (3) the 11-year solar cycle (electron density levels reach a maximum value approximately every 11 years, which corresponds to a peak in the solar flare activities known as the solar cycle peak. 2012 was a peak of solar cycle number 24); and (4) the geographic location (electron density levels are minimum in mid latitude regions and highly irregular in polar, auroral, and equatorial regions). As the ionosphere is a dispersive medium, it causes a delay that is frequency dependent. The lower the frequency, the greater the delay; that is, the L2 ionospheric delay is greater than that of L1. Generally, ionospheric delay is of the order of 5m to 15m, but can reach over 150m under extreme solar activities, at midday, and near the horizon (Elrabbany, 2002)

2.8. TOTAL ELECTRON CONTENT MEASUREMENT (TEC)

Most measurements and applications of total electron content had to do with arbitrary slant ray paths between a satellite and a ground station. However, for relative purposes it is necessary to define the observations in a more standard way. In effect, the pattern was adopted at an early stage to apply a simple geometrical construction, usually based on an assumed thin-shell ionosphere at a defined height, to rotate the actual slant measurement to obtain equivalent vertical total electron content. In practice, most estimates of total electron content (usually abbreviated to TEC and measured in units where (1 TECU $=10^{16}m^{-2}$) are based on this

equivalent vertical parameter (Kersley, 2004). In general, an unknown bias is associated with electron content measurements. There are two methods for treating these biases. The first is to solve for the biases through complex modeling techniques (Coco *et al.,* 1991; Mannucci *et al.,* 1998; Dear and Mitchell, 2006). The second is to treat TEC measurements as relative measurements. In order to convert these relative measurements into an absolute value, it is necessary to provide a baseline.

2.9. TOTAL ELECTRON CONTENT FROM GPS

Total electron content (TEC) is an important descriptive quantity for the ionosphere of the earth. TEC is a very important parameter of the ionosphere for the study of the effects on the signals transmitted by a Geo-positioning system (GPS) satellite to the receiver on the earth. It is therefore a key parameter in the mitigation of ionospheric effects on radio systems. TEC is the total number of electron integrated between two points along a tube often reported in multiple of TEC unit defined as

$$1\text{TECU} = 10^{16}\ \text{e/m}^2$$

TEC is therefore the number of electrons in a tube of 1m^2 cross section extending from the receiver to the satellite (figure 1). TEC along the signal path is then given by

$$TEC = \int_{rec}^{sat} N_e ds \qquad (2.8)$$

Where N_e is the electron density along the signal path

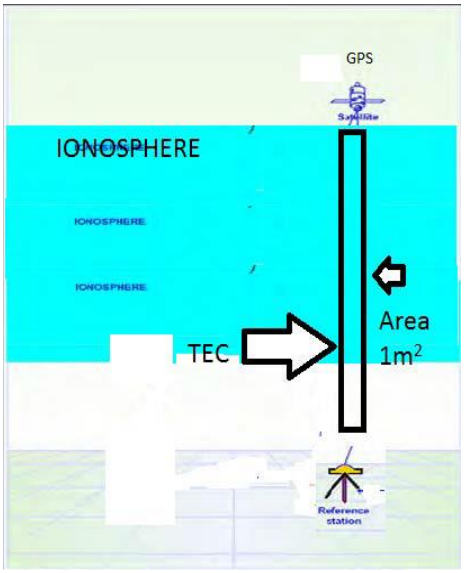

Figure 2.3 TEC as electron density within square meter
Between the GPS and receiver (Source: Rabiu, 2011)

Theoretically, different period of ionospheric physical process can be studied by detecting and examining the temporal variation of TEC. Total electron content is therefore a key parameter in the moderation of ionospheric radio effect, in numerous application involving radio links between satellite and the ground receiver, which play vital roles in the modern technology of communication, navigation and surveillance, the propagation deviates from free space conditions in various ways with significant effects for the accuracy and reliability of the service (Kersley *et al.*, 2004). Usually as found the minimum TEC occurs before sunrise and the maximum TEC occurs between 1:00pm – 5:00pm.

The GPS orbits at an altitude of 20,200 Km with an orbital period of 12h and an orbital inclination of 55^0 to the equator. Each satellite transmits signals at two frequencies of L1 of 1.57GHz and L2 of 1.227GHz. The GPS navigation system comprises of three distinct "segments" (Ackroyd and Lorimer, 1990), of which the first one is the space segment that consists of a constellation of 24 satellites transmitting coded signals downward to receivers on the Earth's surface. The second is the control segment, which consist of four monitored stations and four ground antennas used for monitoring satellites and sending signals upward for the

engineering control of each satellite and its transmitted codes and waveforms. And the third one is the user segment which includes everyone with a GPS receiver who is making use of the transmitted signals. Satellites are equi-spaced around each of the six circular orbital planes inclined at 55^0 to the plane of the Earth's equator. The geometry in the location of the satellite constellation is such that, from any point on the Earth's surface with a reasonably unobstructed horizon, signals from at least four satellites will always be available in the line of sight and it will therefore be possible to solve the four unknowns of the receiver, namely latitude, longitude, altitude and the combined satellite/receiver timing error.

Shastri *et al.* (1996) made a study of the performance of the IRI-90 in the Indian sector from a comparison of foF2 observed at four locations and found that the IRI in general overestimates the observed peak density at all solar activity levels. The difference between observation and prediction varies with local time and location. On the other hand, Iyer *et al*. (1996) have shown that the IRI overestimates TEC during low solar activity and underestimates it in high solar activity at the crest of the anomaly both in the Indian and East Asian longitude sectors. Bhuyan and Chamua. (2002) have compared the electron density predicted by the IRI- 1995 at the height of 600 km in the 75^0 E longitude sector with the electron density measured by the Hinotori satellite within $\pm 25^0$ of the geomagnetic equator. They found that the model underestimates the observed electron density in all seasons and at about all local times during moderate and high solar activity. (Bhuyan *et al.*, 2007) compared TEC obtained from GPS locations with that predicted by the International Reference Ionosphere 2001 to assess its predictability in the Indian equatorial and low latitude sector It was found the IRI 2001 overestimates TEC throughout the year and at about all local Times. The solar ionizing radiation flux, magnetic activity and transport of ionization under the influence of neutral winds and diffusion are some of the principal factors that affect the level of ionization in the ionosphere, which is also reflected in the integrated total electron content at any given location.

Earlier studies have revealed that the 'noon time bite-out' at or near the magnetic equator shows a marked dependence on longitude.

Prassad, *et al.* (2011) studied TEC variability over Indian low latitude sector and the result was compared with IRI 2007 model. The GPS derived TEC data over four different latitudes in the Indian region are used to study the diurnal, day-day and seasonal characteristics of TEC. The diurnal behavior of TEC has shown a short lived day minimum with a broad day maximum over Trivandrum and Waltair with the night time maintenance of ionization. The day maximum values of TEC are higher over Waltair and Bhopal (close to EIA crest) compared to those at Trivandrum (Equatorial station) and Delhi (located outside the EIA crest). The TEC values are higher during equinoctial months and lower during summer months. A significant day-to-day variability is observed and it is more at the anomaly crest locations and less at the equatorial station. Study of ionospheric variations of the vertical VTEC at low-middle ionosphere shows dependence on solar activity. The study of ionospheric total electron content has been done by a number of workers in Africa(Ngwira *et al*., 2012; Oladipo *et al*., 2008; Adohi, *et al*., 2008; Ouattara *et al*., 2009, 2012; Obrou, *et al*. 2009; Adebiyi *et al*., 2014; Ouattara and Amory-Mazaudier, 2012; Rabiu *et al*., 2014; Shimeis *et al*., 2014). Ouattara and Mazaudier. (2012) showed that the different types of solar activity occurring during the different phases of solar cycle modified the diurnal pattern of ionization. They used the classification of Legrand and Simon. (1989) made on one century (1868–1978) of geomagnetic activity (Legrand and Simon, 1989).These classes related to solar activity are: (1) the magnetic quiet activity due to slow solar wind flowing around the magnetosphere, (2) the recurrent activity related to high wind speed solar wind, (3) the fluctuating activity related to fluctuating solar wind and (4) the shock activity due to shock events (CME). Forbes *et al*. (2000) investigated the variability of the ionosphere and observed that ionosphere increased as magnetic activity increases from lower to higher latitudes. Rabiu et al. (2007) examined the variability of the equatorial ionosphere

inferred from geomagnetic field measurement and made the following submission: equatorial electrojet exhibits diurnal variations on both quiet and disturbed days throughout the year; the daytime magnitude of the solar daily variation in magnetic field is greater than the nighttime magnitudes for all the months.

2.10. THE IRI MODEL

In order to establish an international standard for the specification of ionospheric parameters based on worldwide available data from both satellite and ground station observations, the Committee on Space Research (COSPAR) and the International Union of Radio Science (URSI) created the International Reference Ionosphere (IRI) project in the late 1960s. Its main goal was to build an empirical model to avoid the uncertainties developing in the theoretical understanding of ionospheric processes and coupling to the regimes observed below and above and also in establishing a standard representation of the plasma parameters in Earth's ionosphere. The IRI model is an internationally accepted standard model for the estimation of ionospheric parameters (e.g., electron density, total electron content, electron and ion temperature, and ion composition), which can be derived as a function of geographic location, time (LT or UT), height and sunspot number for magnetically quiet days. The IRI model has been improved over time with the addition of data from worldwide ground stations and satellite observations (Bilitza, 2003). Earlier models have mainly successfully focused on mid- latitude regions. However, many researchers found an under- or over-estimation of the modeled TEC for equatorial and low- to mid-latitude regions (Bhuyan and Borah, 2007.). Such a model of the ionosphere is important for many applications that rely on electromagnetic waves traveling through the ionosphere including telecommunication, GPS, earth observation from space (e.g., satellite altimetry), radio astronomy and many more, because all of these applications need to correct for the retarding and refractive effect of the ionosphere on the probing signal. The latest version of the IRI model, IRI-2012, includes several important improvements and new

additions that lead to a more accurate representation of (1) the electron density and ion composition in the region from the F2 peak down to the E peak, (2) the solar cycle variation of the electron temperature, (3) the storm effects in the auroral E-region, and will for the first time include the representation of auroral oval boundaries and their magnetic storm (Bilitza, 2014) induced movement to lower latitudes (4) The IRI-2012 version, also includes an additional number of indices such as the 3-h Ap - index, the daily Ap-index, the 3-h Kp - index, and the 81 days solar radio flux $F_{10.7}$ 81D(Arunfold *et al*, 2014.). More information on the IRI project can be found on the IRI home page at http://IRI.gsfc.nasa.gov/. The observed values of VTEC are compared with the values modelled by the IRI-2012. IRI is an empirical ionospheric model based on experimental observations of the ionospheric plasma. The IRI model describes monthly averages of the electron density, electron temperature; ion composition, ion temperature, and ion drift in the current altitude range of 50–2000 km (Adewale, *et al* 2012; Rabiu *et al.,* 2014). The accuracy of the IRI model in a specific region and/or time period depends on the availability of reliable data for the specific region and time since it is a data-based model (Bilitza, 2014). Daily TEC at 2000km is selected as the upper boundary of electron density profiles and the model provides the option for the bottom side electron density shape parameter.

CHAPTER THREE

METHODOLOGY

3.1. PROCEDURE OF DATA COLLECTION

The GPS data, for the year 2012 is used for TEC variability and validation of IRI 2012. The GPS network is termed NIGNET (NIGerian GNSS Reference NETwork) (Rabiu et al., 2014). The GPS data is in Receiver Independent Exchange (RINEX) format. RINEX is data interchange format for raw satellite navigation system data. The coordinates of the two stations used for this study are given in Table 1. The RINEX observation files were processed by the GPS-TEC analysis application software, developed by Goppi Seemala of the Institute for Scientific Research, Boston College, USA.

3.2. DATA COLLECTION

TEC can be obtained from the ionospheric delay between L1 and L2 signals as shown in Eqn. (2.3). Hence the GPS frequencies L1 (1575.42 MHz) and L2 (1227.6 MHz) experience different group delays and phase advances as shown in equations. (3.1) and (3.2). TEC from group delay, using pseudo-range measurements, (Rabiu *et al.,* 2014) is given by

Table 3.1 Geographic and Geomagnetic stations

Station Code	Location	Geographic		Geomagnetic	
		Longitude	Latitude	Longitude	Latitude
BKFP	Kebbi state	4.299	12.649	76.62	0.72
ABUZ	Zaria	7.649	11.152		

$$\text{TEC}_g = \frac{1}{40.3}\left(\left(\frac{1}{f_1^2}\right) - \frac{(1)}{f_2^2}\right)^{-1} \times (p_1 - p_2) \quad (3.1)$$

Where f_1 and f_2 are L1 and L2 carrier frequencies, and P1 and P2 are pseudo-range observables. TEC from carrier phase measurements is given by

$$TEC_p = (c_1 - c_2) \times 2.852 \qquad (3.2)$$

Where C1, C2 are C/A and L2C code measurements.

Calculation of TEC from group delay measurement is absolute and noisy. The relative phase delay between the two carrier frequencies gives a more precise measure of relative TEC, but is ambiguous because the actual number of cycles of phase is unknown. The ambiguity term is resolved by combining the two estimates of TEC Eqns. (3.1) and (3.2) to form an improved estimate of absolute TEC (Rabiu et al., 2014.). The GSV 4004 Ionospheric Scintillation Monitor receivers (ISMs) collect the TEC and scintillation data (Rama Rao *et al.*, 2006). Each ISM can track up to 11 GPS C/A-code signals at the L1-frequency of 1.575 GHz. The data is collected at one minute intervals from all the stations, which do not include the 50-Hz sampled raw data, but the reduced TEC and S_4 index and other parameters are included. TEC data, recorded at the 2 different locations during the twelve-month period, from January 2012 to December 2012, is used in this analysis. Here, The Slant TEC (STEC) records from GPS are polluted with satellite differential delay, b_S (satellite bias), and receiver differential delay, b_R (receiver bias), joined with receiver inter-channel bias (b_{RX}). This uncorrected STEC measured at every 1 min interval from the GPS receiver derived from all the visible satellites at the two stations are converted to vertical TEC (VTEC). VTEC can be expressed as (Bolaji *et al.*, 2012; Rama Rao *et al*., 2006)

$$VTEC = STEC - [b_R + b_S + b_{RX}]/S(E) \quad (3.3)$$

where STEC is the uncorrected slant TEC measured by the receiver, S (E) is the obliquity factor with zenith angle, Z, at the ionospheric pierce point (IPP), E is the elevation angle of the

satellites in degrees, and VTEC is the vertical TEC at the IPP .To eliminate effect due to multipath, a minimum elevation angle of 20° is used (Bolaji *et al*., 2012; Rama Rao *et al.*, 2006). The VTEC data estimated are then subjected to a-two-sigma (2s) iteration, which are a measure of GPS point positioning accuracy (95% confidence level). This 95% confidence level corresponds to 1.96 standard deviations, which is then approximate to two standard deviations or 2s, and the resulting values are the average of VTEC over all pseudorandom numbers (PRNs) on a day. In addition to eliminating the errors from multipath, the satellite and receiver biases were removed from the TEC values used in this present study. The satellite and receiver bias values were obtained from the data Centre of Bern University, Switzerland. S (E), which is the mapping function, is defined as (Mannucci *et al*., 1993, 2002; Bolaji *et al.*, 2012)

$$S(E) = \frac{STEC}{VTEC} \qquad (3.4)$$

$$\text{S (E)} = \frac{1}{COS(Z)} = \left\{1 - \left(\frac{R_E \times COS(E)}{R_E + h_s}\right)^2\right\}^{-0.5} \qquad (3.5)$$

Where R_E is the mean radius of the Earth in km, h_S is the effective height of the ionosphere above the Earth's surface and is approximately equal to 350Km, z is the zenith angle and E is the elevation angle in degrees.

The vertical TEC (VTEC) thus calculated is used in deriving the results. The average 1 min VTEC data was extracted manually into Microsoft excel for analysis, the diurnal variation was studied by averaging the one minute data to hourly values throughout the year. The usual time convention for ionospheric data analyses is in universal time (UT), but for this study local time (LT) is used because variation in TEC is location-dependent. Nigeria is 1 h ahead of universal time so the universal time (UT) data are converted to local time (LT). Seasonal variation of VTEC were investigated by classifying the months into different seasons based on the

movement of the sun by averaging the sunspot number (R_Z =57.58) for the year 2012 shown in table 2, which is a year of moderate solar activity.

S/NO	Months	Sun spot number
1.	January	58.3
2.	February	32.9
3.	March	64.3
4.	April	55.2
5.	May	69
6.	June	64.5
7.	July	66.5
8.	August	63.0
9.	September	61.4
10.	October	53.3
11.	November	61.8
12.	December	40.8

For this study the classification of Rabiu *et al*. (2011) was followed: March Equinox (MAREQUI) comprising: February, March, April. June Solstice (JUNSOLS): May, June, July. September Equinox (SEPEQUI): August, September, October, and December Solstice (DECSOLS): November, December, January, for the year 2012. To further expand the research work, a second classification was considered according to geomagnetic classification: Winter, summer and Equinox and the VTEC for the two stations during this period were also evaluated. The final result is compared with the IRI model 2012.

To quantify the performance of the model a root mean square error (RMSE) has been used. This was evaluated for Birnin Kebbi (BKPF), Zaria (ABUZ) and the IRI Model using the equations (3.6 – 3.7):

$$\text{RMSE}= \sqrt{\sum_{i=1}^{N} \frac{1}{N} (VTEC - IRI)^2} \qquad (3.6)$$

$$\text{RMSE } = \frac{1}{N} \sum_{i=1}^{N} (RMSE)_i \qquad (3.7)$$

Where N is the number of data points.

CHAPTER FOUR

RESULT AND DISCUSSIONS

4.1. MONTHLY VARIATION IN TEC

The graphs below (Figures 4.1and 4.2) shows the monthly variation in TEC for Zaria and Birnin Kebbi Polytechnic from January to December 2012 in the two selected stations.

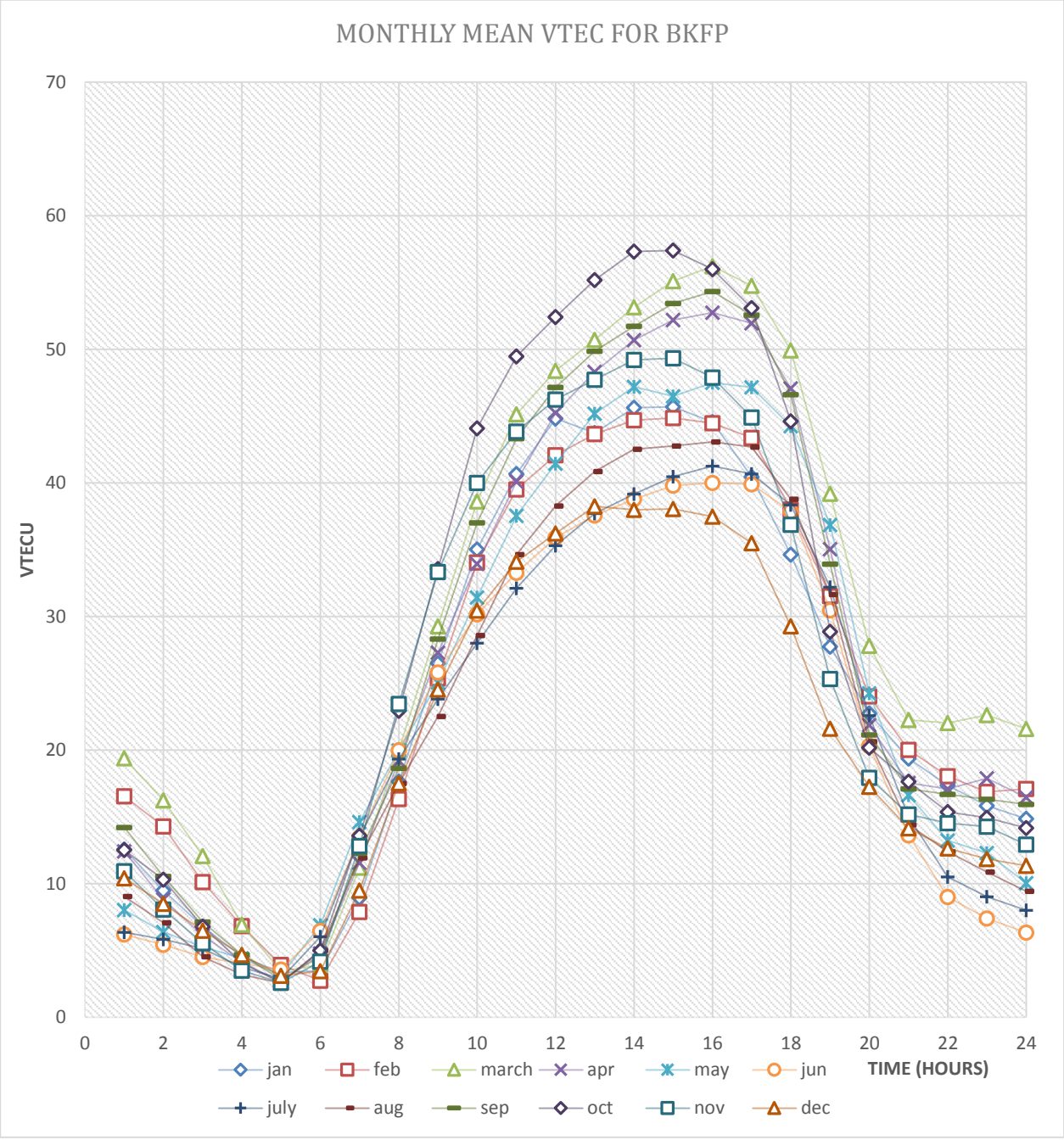

Figure 4.1: Monthly Mean VTEC for Birnin Kebbi (January – December, 2012)

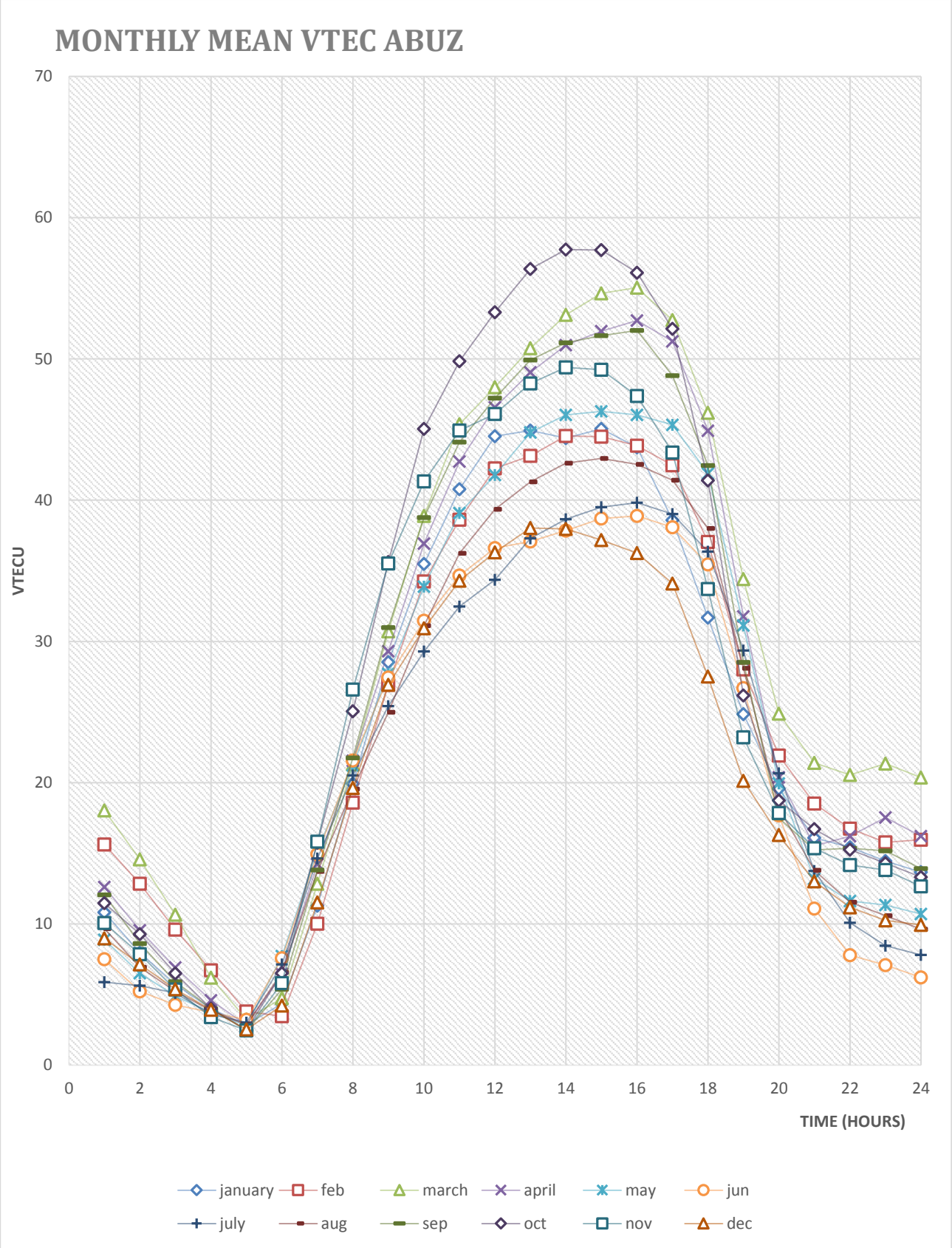

Figure 4.2: Monthly Mean VTEC for ABU Zaria (January – December, 2012)

4.1.1. DISCUSSIONS

It was found that characteristics of TEC are dependent primarily on the position of the station with respect to the magnetic equator.

Monthly variations of vertical total electron content (VTEC) have been studied by plotting the monthly mean of VTEC of the year 2012 as shown in Figures 4.1 and 4.2 respectively for the two selected stations. The plots show that VTEC has higher values during daytime compared with nighttime values, over all the stations and in all the months. The daily peak values of the VTEC occurs around 14:00 to 17:00 LT. The curves shows there is considerable day-to-day and month to month variations of TEC derived from different satellite passes, particularly, during the mid-day to pre-dawn hours which is a serious concern in forecasting and navigation (Bagiya *et al*., 2009; Rama Rao *et al*., 2006). Observations at the two stations showed that the VTEC values are high in October with highest TEC of ~58TECU occurs around 15:00LT, followed by march September and April with highest TEC of ~56, ~54 and ~52TECU respectively occurred around 15:00 to 16:00LT. VTEC values are low in December with highest TEC of ~38TECU, compared to the other months. During the daytime, the equator is hotter than the North and South poles. This causes meridional wind flows towards the poles from the equator. As reported by Balan *et al*. (2000) and Bagiya, *et al.* (2009), this flow of meridional wind changes the neutral composition and O/N_2 decreases at equatorial stations. This decrease in O/N_2 ratio, which is, maximum during the equinox months, will result in higher electron density. Hence equinox VTEC will be highest as found by our result. The day-to-day variations of TEC may be attributed to the changes in solar activity which is associated with changes in the intensity of the incoming radiations (Fayose *et al*., 2012). The diurnal variation in TEC shows that the time at which TEC attains maximum vary from day to day. Large variations of TEC are observed in daytime while nighttime variations are found to be almost constant. VTEC values generally increase from 0600 LT for all the months and reach a

maximum value during 1500–1700 LT. In addition, VTEC exhibits the usual diurnal variation of a minimum in the pre-sunrise hours (0500 LT) with a minimum TEC of ~3TECU at all the stations and months. These diurnal monthly variations are caused by Extreme Ultraviolet flux, geomagnetic activity, equatorial electrojet and local atmospheric conditions in the thermosphere (Rabiu, *et al*., 2014; Bagiya, *et al*., 2009). From all the months, the maximum DTEC daytime magnitude range is between ∼38 and ∼58 TECU, It is clearer that the range is maximums during daytime. VTEC in all the months is greater than the minimums range observed at nighttime (post sunset and pre sunrise) magnitude range of 5TECU to 28TECU. This greater magnitude of VTEC during daytime is attributed to solar EUV ionization coupled with the upward vertical E × B drift. These results are in agreement with the results obtained at the equatorial region by (Rama Rao *et al.*, 2006; Liu *et al*., 2009; Bolaji *et al*., 2012; Rabiu *et al*., 2012; Olawendo *et al.*, 2012). They concluded that the upward drift velocity can lift the ionosphere to higher altitudes where the ionization loss rate is smaller. They attributed this phenomenon to chemical loss of the daytime fountain effect at the magnetic equator. They further suggested that in hastening this chemical loss during daytime, regular chemical decay is augmented by downward driven motions of both pole ward and zonal (eastward) neutral wind blowing away the fountain effect from the equator at noon until afternoon.

4.2. SEASONAL VARIATION

The graphs (Figures 4.3 and 4.4) shows the seasonal variation of TEC for the two stations using geographic seasonal classification, while (Figures 4.5 to 4.6) are also seasonal variation using geomagnetic classification of seasons

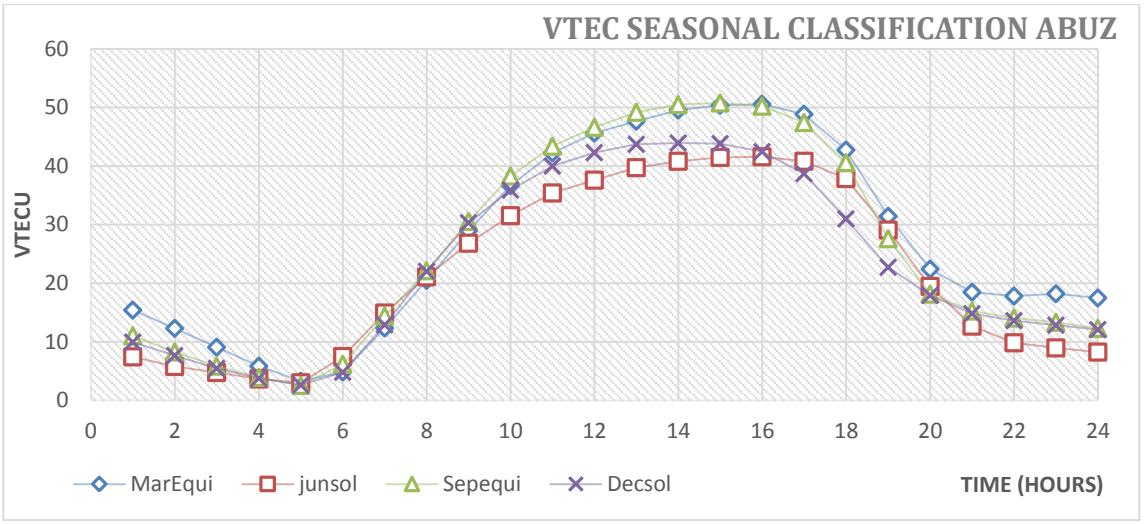

Figure 4.3: Seasonal Variation for VTEC at ABU Zaria GPS Station

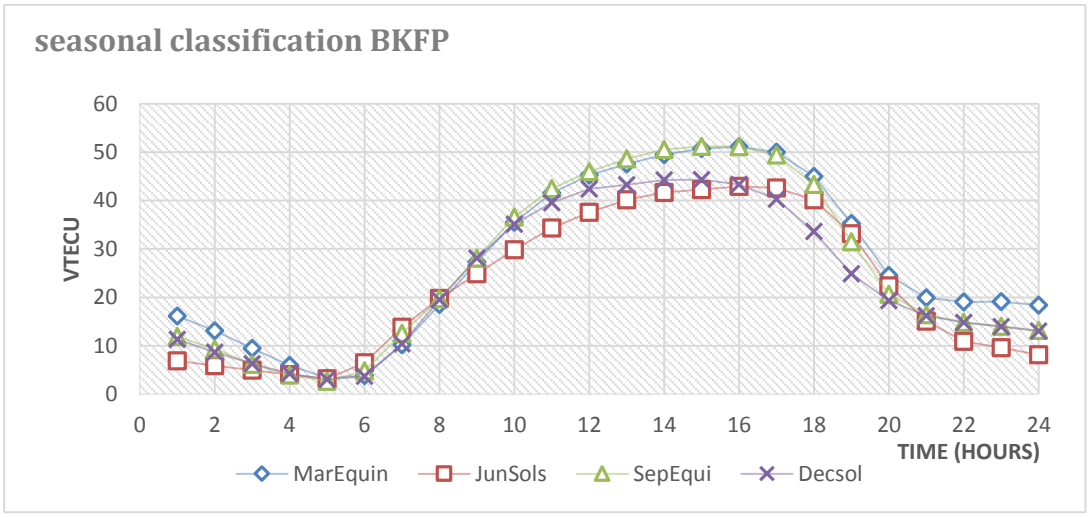

Figure 4.4: Seasonal Variation for VTEC at Birnin Kebbi GPS Station

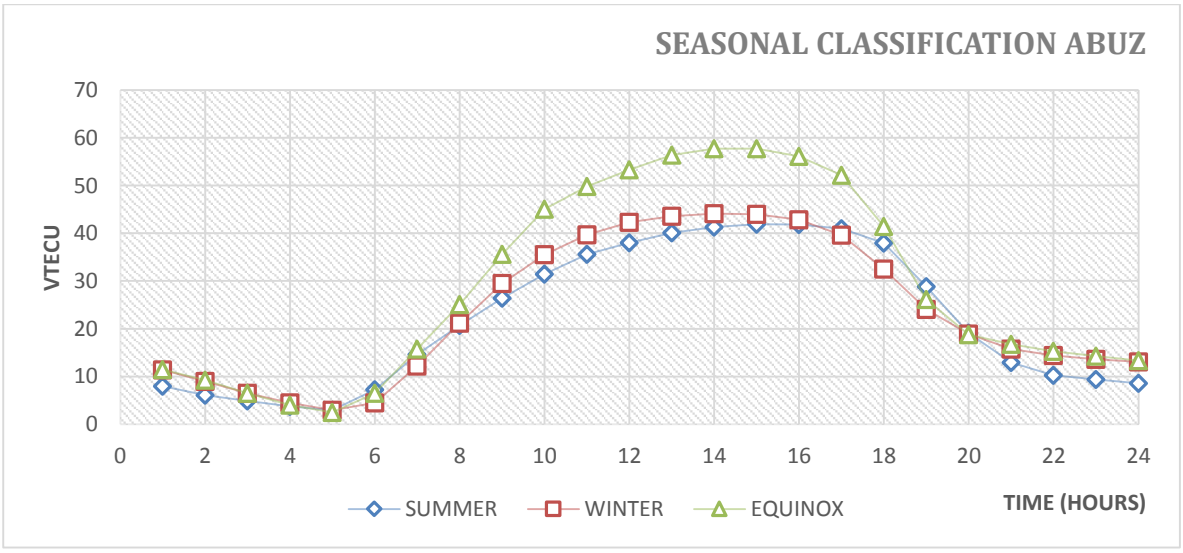

Figure 4.5 Seasonal Variation of VTEC at ABUZ GPS station

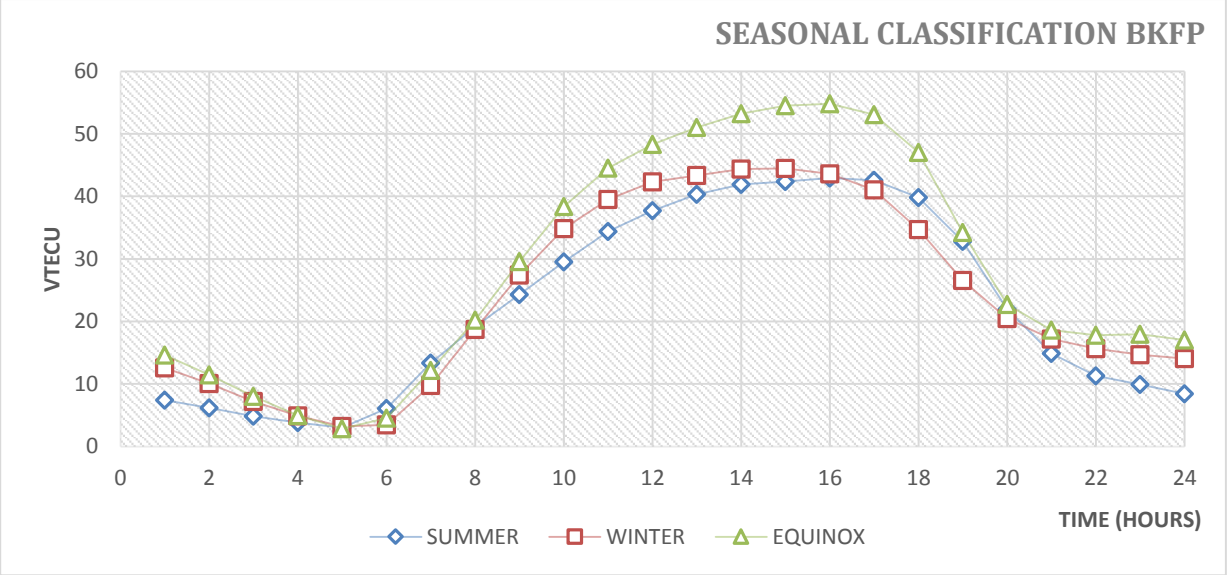

Figure 4.6 Seasonal variation of VTEC BKFP GPS station

4.2.1. DISCUSSIONS

The ionosphere exhibits strong seasonal and solar cycle variations because the main source of ionization and energy for the ionosphere is photo ionization. Therefore, whenever either the solar zenith angle or the solar radiations flux change, the ionosphere dynamics may reflect these changes. The ionosphere's seasonal variations is related to solar zenith angle change, while its solar cycle variation is related to a change in solar EUV and X-ray radiation fluxes (Schunk and Nagy, 2009; Kelley, 2009). The seasonal variation is investigated by averaging the hourly values for all days of the season. The GPS–TEC analysis soft- ware gives an output in an ascii files which contains Slant TEC (STEC) and VTEC calculated at IPPs during the satellite pass. The mean daily hourly VTEC are obtained by averaging all the observations at a particular hour at different IPPs for all satellite in view. The mean daily hourly VTEC are then summed for all the days of the season and averaged over the number of days within the season to give the mean hourly seasonal values. It is clearly shown from the plots that VTEC has highest value in September equinox (51.188TECU) around 15:00LT followed by march equinox with highest TEC of 51.14TECU in the hours of 1600LT and the lowest magnitude of VTEC is observed in June solstice (42.92TECU) around 16:00LT in BKFP so also the same

pattern is observed in ABUZ station with a highest amplitude of 50.769TECU early 1500LT in September equinox followed by march equinox with TEC of 50.53TECU occurred in the hours of 1600LT and lowest amplitude of 41.58 TECU around 1600LT in June solstice ,this mean that highest electron density is observed in equinoxes the 'winter anomaly in seasonal variation is observed. The time of occurrence of the diurnal maximum also varies with season. TEC reaches its daytime peak earlier (1400 LT) at the December solstice and later (1500 LT) at the June solstice. Since VTEC is lowest in the June solstice for both stations. This is a unique finding since as expected, it is in the equinoxes when the subsolar point is around the equator that there is high photo-ionization which produce more electrons and therefore enhancing the background electron density which results into maximum VTEC during the season (Wu et al., 2004). On the other hand during the solstices, photo-electrons at the equator decrease because the subsolar point moves to higher latitudes and other factors driving the equatorial TEC maximization such as the fountain effect are expected to wane. Rabiu, et al. (2007) attribute the seasonal variation to the electrodynamics effect of local winds since winds are subjected to day to day and seasonal variation. The study of geomagnetic classification of season into summer (May, June, July, August), winter (November, December, January February) and equinox (March, April, September, October). As recent studies (Pham et al., 2011) showed a large symmetry between the two equinoxes, this study has investigated the two equinoxes separately. This separation is also consistent with the seasons given by the zonal mean circulation of winds in the thermosphere. The winds are flowing from the summer to the winter during summer times and reverse during winter times The values of diurnal peak in VTEC is maximum during the equinox months which occurs around 16:00LT (~55TECU) in TEC and minimum around 05:00 to 06:00 LT (~3 TECU) in TEC, and TEC is higher (44.478TECU) in winter than the summer (42.90TECU) months with maximum occurrence around 15:00 00 LT in TEC minimum of (3.23 TECU) and (3.05TECU)occurred at 0500 LT in BKFP respectively

so also the same in ABUZ station with a highest TEC of 57.75TECU in equinox around 1400LT and the lowest TEC density is in the summer months (41.86TECU) around 1500LT .The VTEC exhibit winter anomaly this effect is caused by seasonal changes in neutral gas composition and suggested that is due to the increased in O/N_2 the vertical wind are down ward in winter resulting in increased of O/N_2 ratio and upward in summer, Consequently, recombination is weaker in the winter hemisphere, leading to higher electron concentration in the winter solstice than that in the summer solstice. Further, Earth's magnetic field is believed to guide plasma from the summer to the winter hemisphere.

4.3. Comparison of GPS-TEC with IRI model derived TEC

The comparisons of experimental VTEC with VTEC of the IRI model are shown in Figures 4.7 and 4.8 for monthly comparison and Figures 4.9-4.14 are for seasons and 4.15-4.21 geomagnetic seasonal classifications.

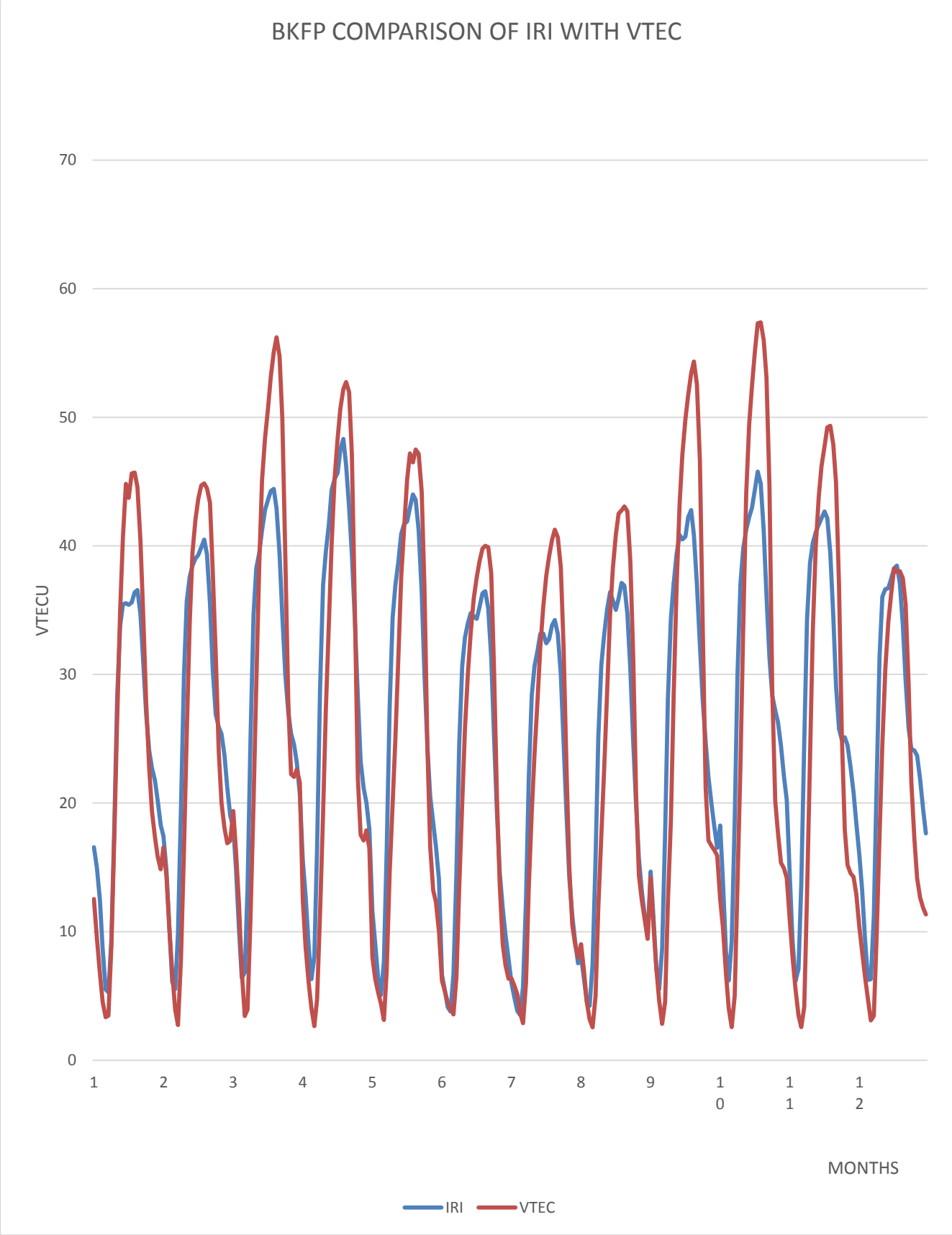

Figure 4.7 comparison of VTEC with the IRI model 2012 for BKFP (January to December 2012

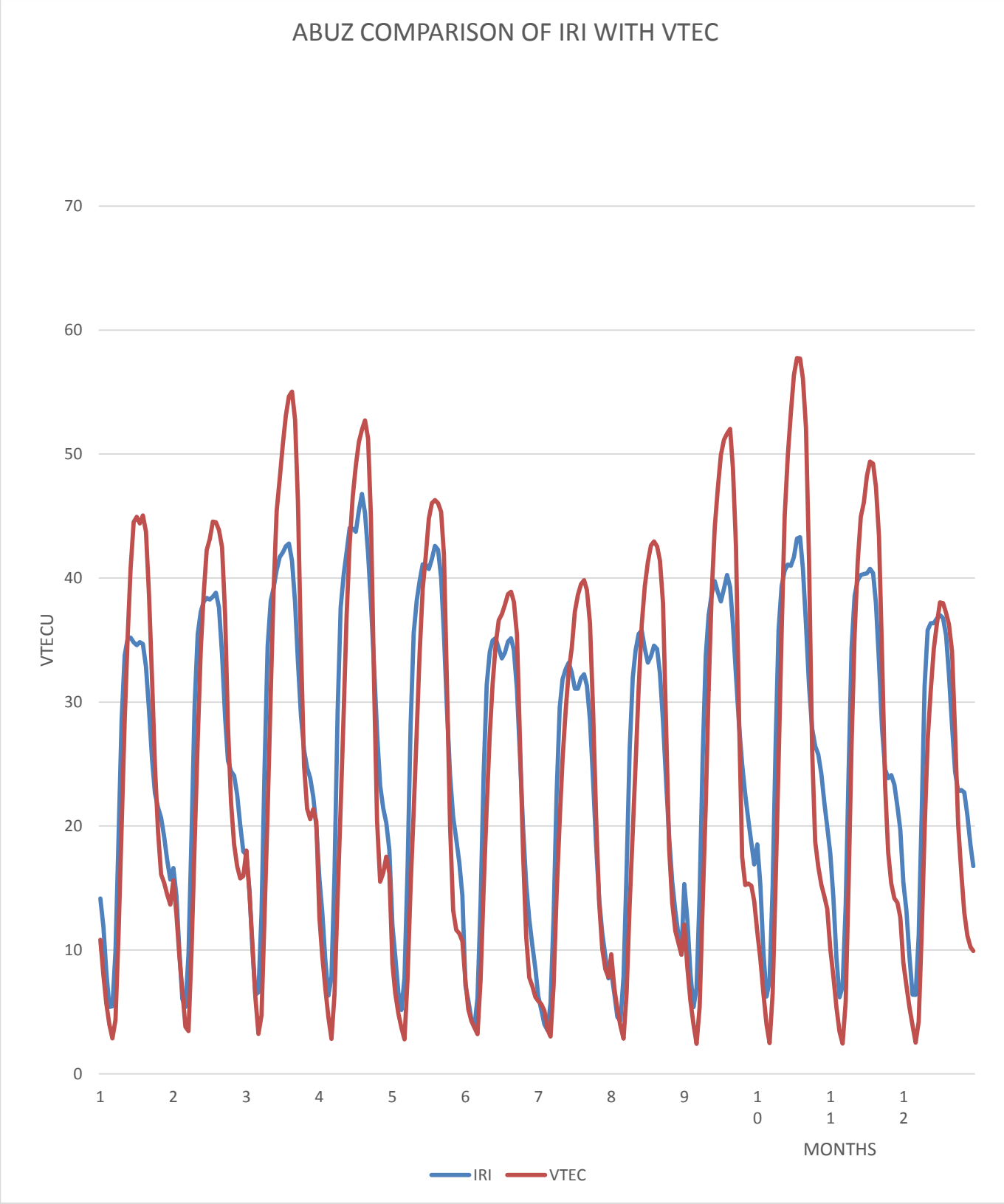

Figure 4.8 comparison of VTEC with the IRI model 2012 ABUZ (January to December 2012)

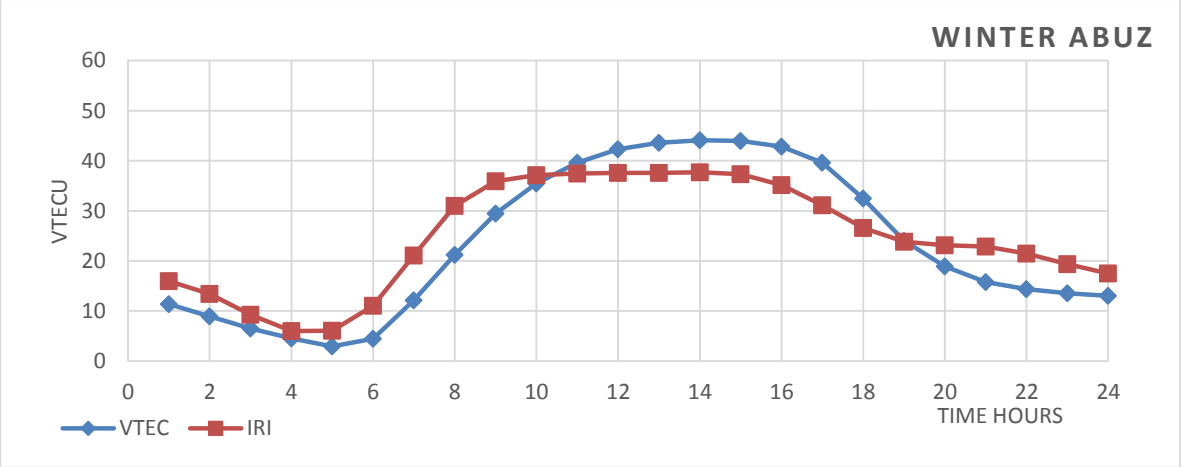

Figure 4.9 Derived VTEC In *Comparison With IRI-Model Winter (2012)*

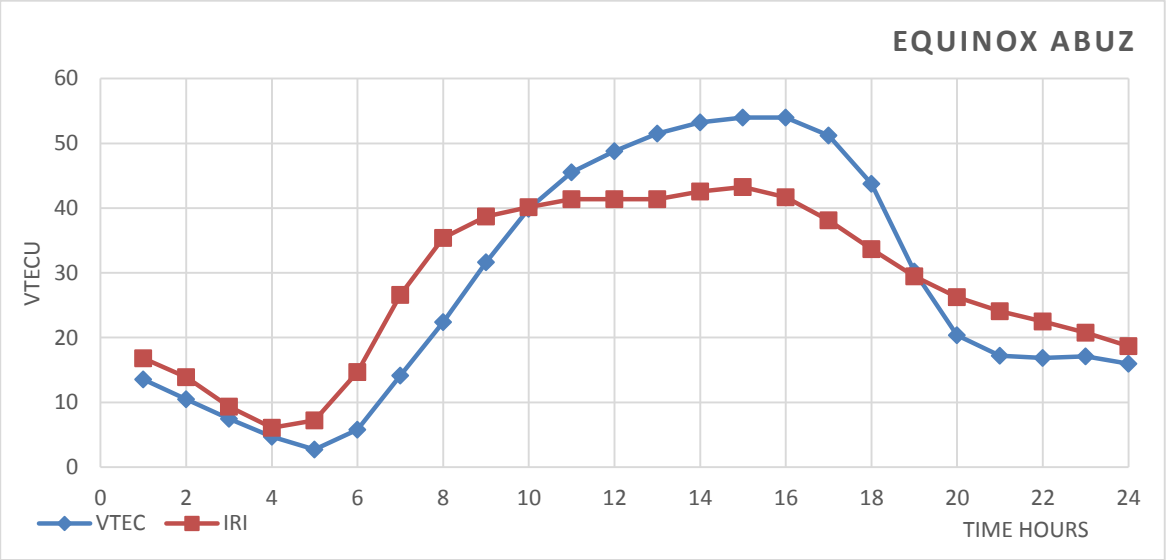

Figure 4.10 Derived VTEC In *Comparison With IRI-Model Equinox (2012)*

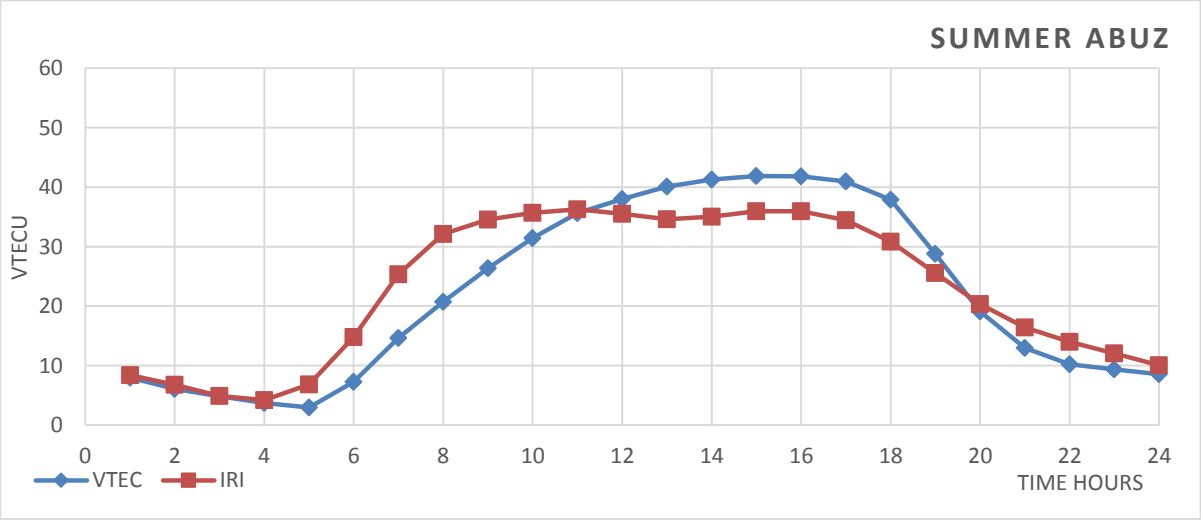

Figure 4.11. Derived VTEC In *Comparison With IRI-Model Summer(2012)*

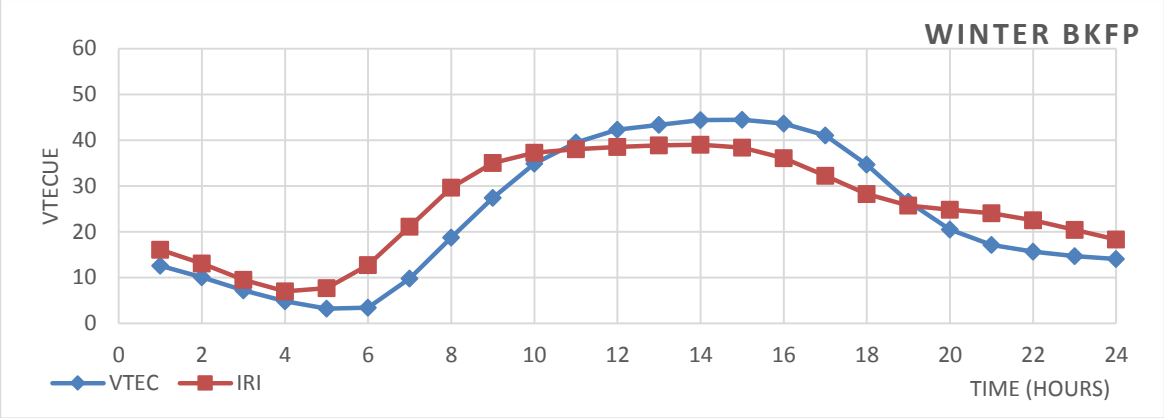

Figure 4.12.Derived VTEC In *Comparison With IRI-Model Winter (2012)*

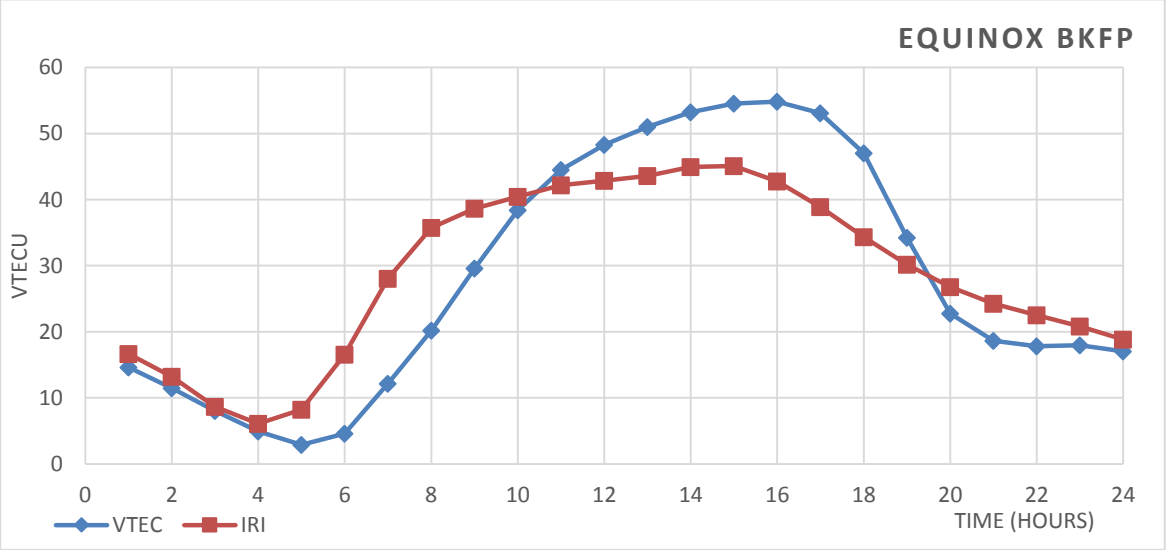

Figure 4.13 Derived VTEC In *Comparison With IRI-Model (2012)*

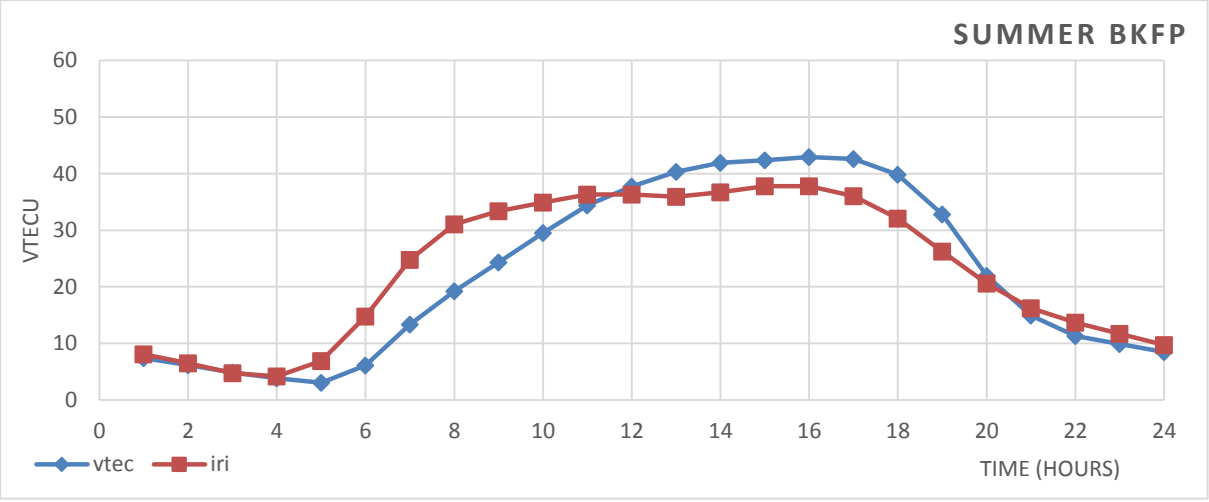

Figure 4.14 Derived VTEC In *Comparison With IRI-Model (2012)*

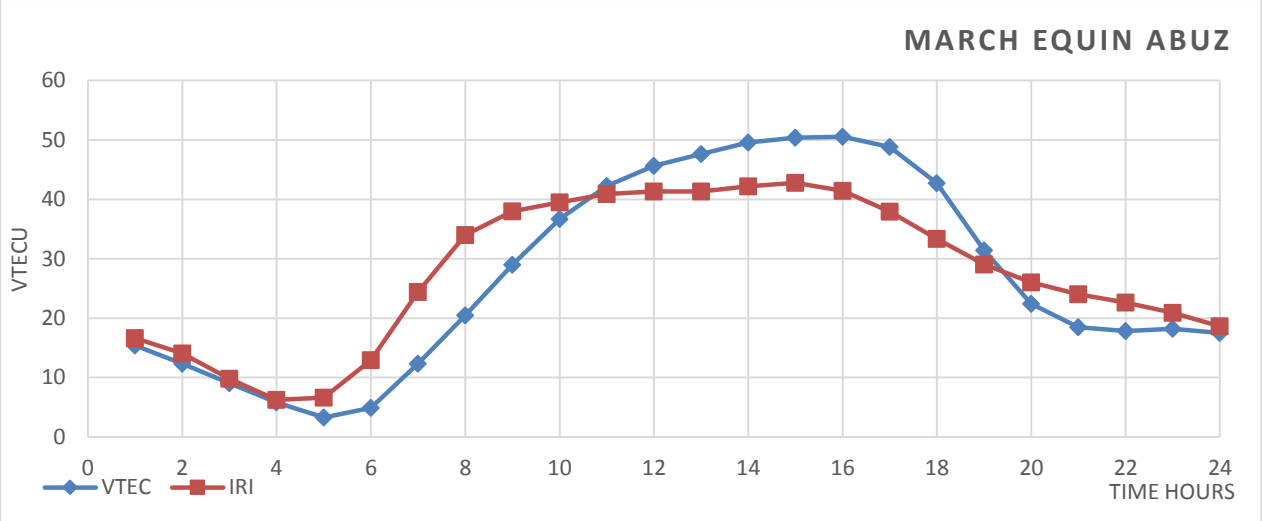

Figure 4.15 Derived VTEC In *Comparison With IRI-Model (2012)*

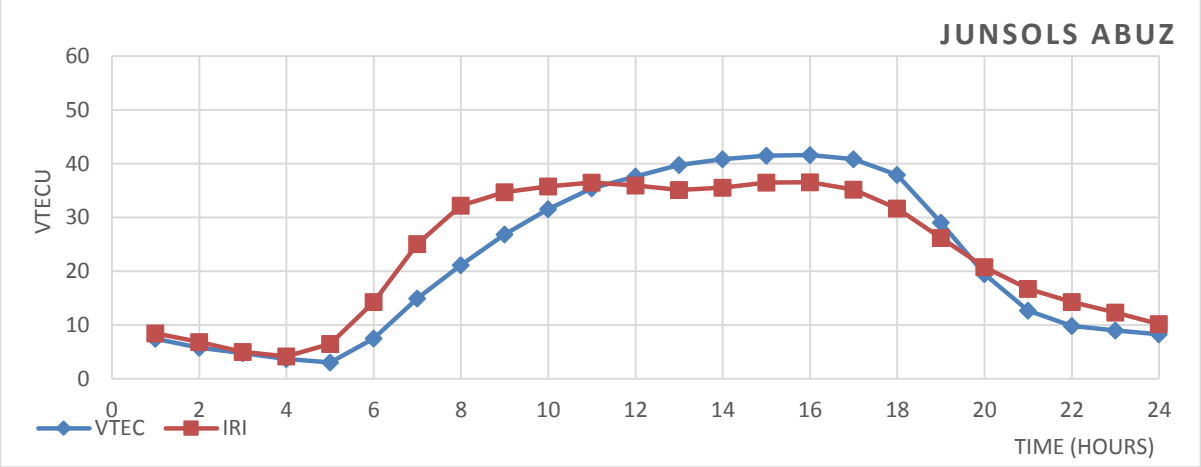

Figure 4.16 Derived VTEC In *Comparison With IRI-Model (2012)*

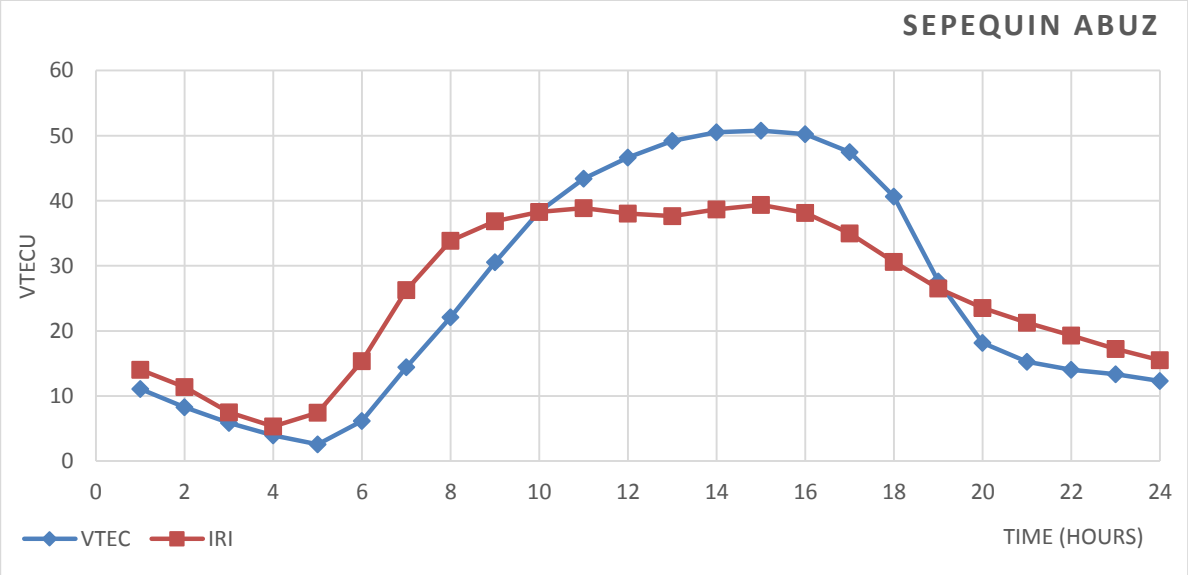

Figure 4.17 Derived VTEC In *Comparison With IRI-Model (2012)*

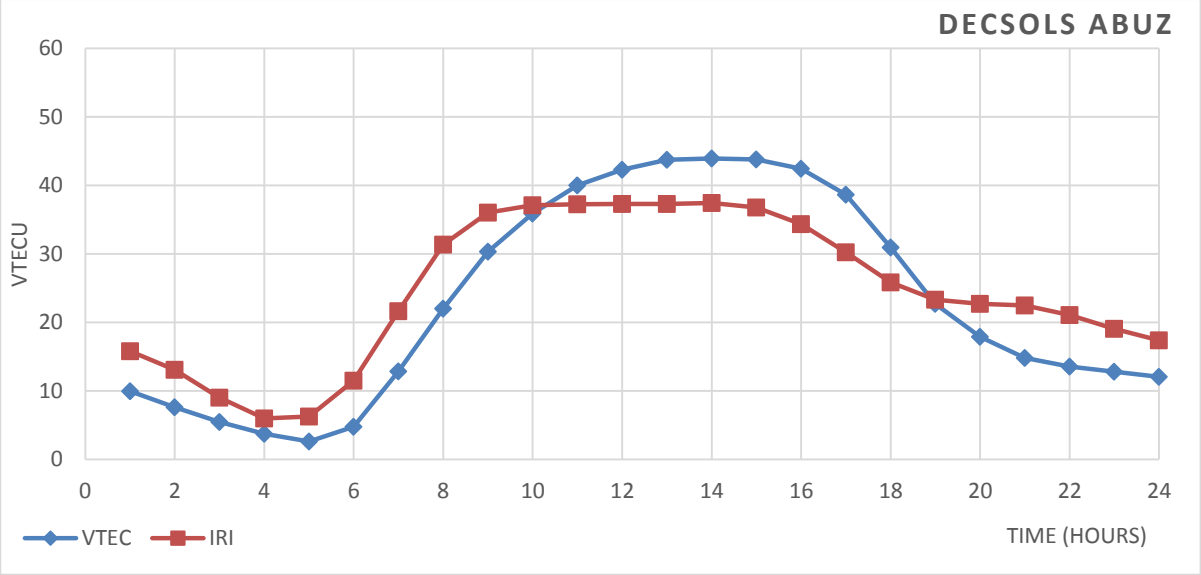

Figure 4.18 Derived VTEC In *Comparison With IRI-Model (2012)*

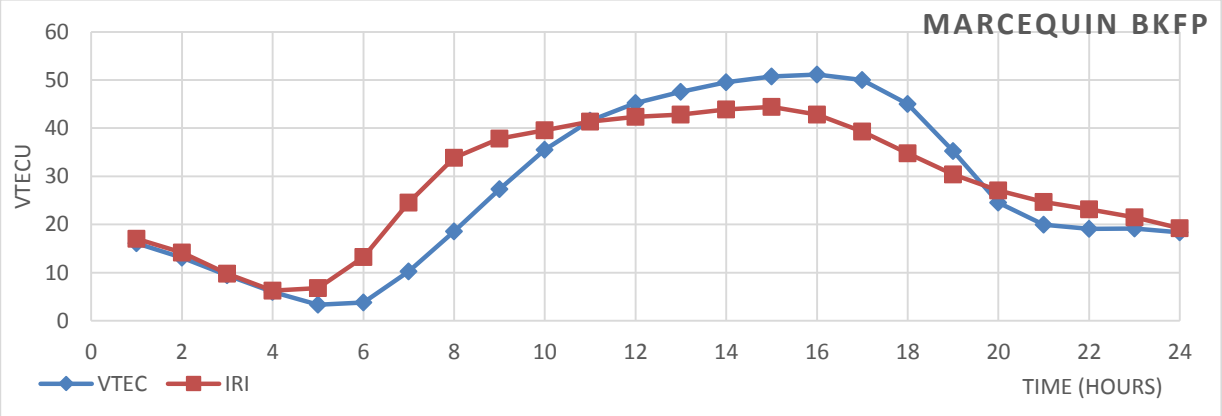

Figure. 4.19 Derived VTEC In *Comparison With IRI-Model (2012)*

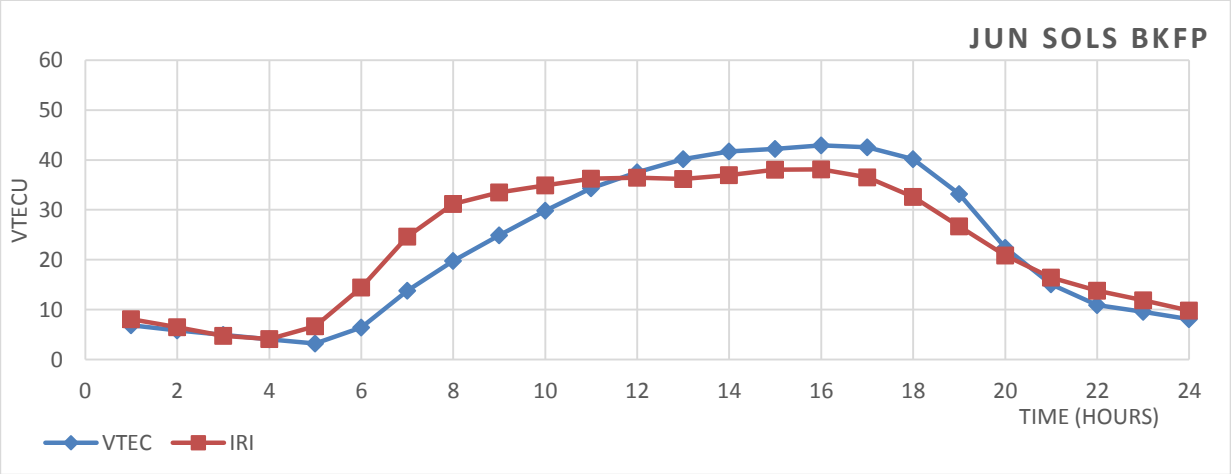

Figure 4.20 Derived VTEC In *Comparison With IRI-Model (2012)*

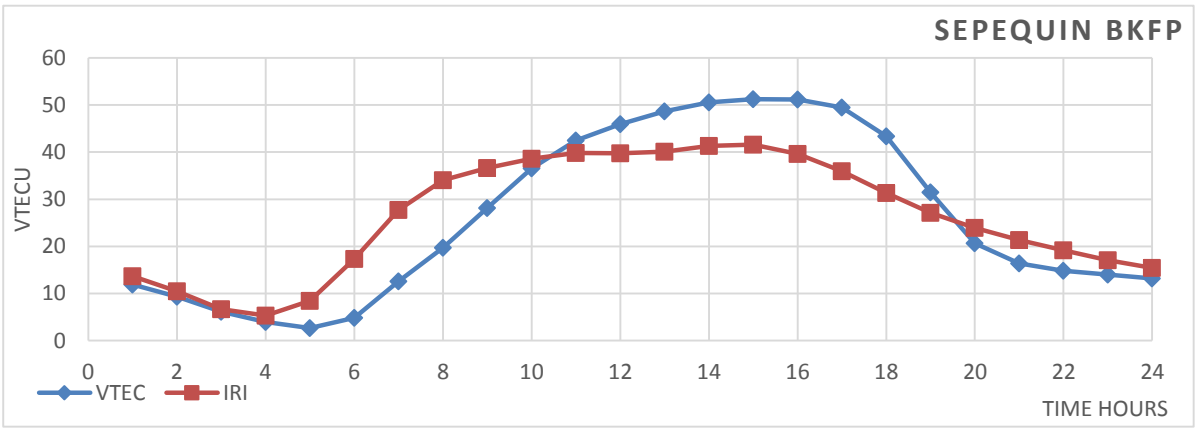

Figure 4.21 Derived VTEC In *Comparison With IRI-Model (2012)*

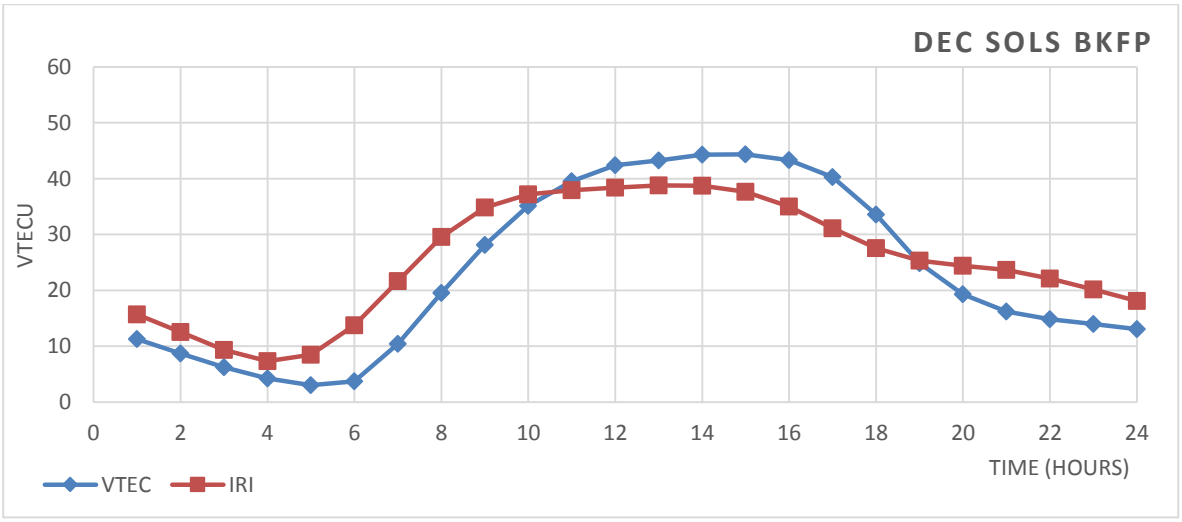

Figure 4.22. Derived VTEC In *Comparison With IRI-Model (2012)*

4.3.1. DISCUSSIONS

The monthly and seasonal trends noticed in both the model and observed data are in good agreement. However, during the daytime the models show an under estimation in all the months and seasons and at the two stations. The IRI plot is closer to the observed VTEC during the nighttime at the two stations and in all the months with a TEC difference of 3TECU to 4 TECU which occurs between the hours of 24:00 to 4:00 LT and a large difference in TEC is observed in daytime between the hours of 1300LT to 1700LT in all the months and seasons with different occurrence of TEC during the day with a TEC difference of 6TECU to 10 TECU in all the months and at all the seasons and in both the two stations. The model TEC is closer to the observed VTEC during the sunrise and sunset compared to the day time, in the months of January BKFP, the IRI model matches the GPS derived TEC between the hours of 6:00 to 10:00 LT and also in the months of February, March, June, July, August between the hours of 24:00 to 4:00 LT. The TEC values increased, likely due to the increase in solar activity and proximity of solar cycle 24. During sunrise, both models exhibited good correlation with GPS-TEC data. However, at noon the model underestimated TEC during all the months and seasons after sunset, the IRI-2012 model exhibited little overestimation, or matches the GPS derived TEC, from all monthly and seasonal plots, it can be inferred that the TEC was higher during equinox periods than during solstice periods, in agreement with earlier studies. The larger difference between the GPS-TEC and the IRI-modeled TEC around noon indicates that the ionosphere in this two stations or in the equatorial area expands during this period, becoming thicker. At equatorial latitudes, the steepest gradients, sharpest peaks, deepest troughs, and density crests occur on both sides of the equator, as explained by Bilitza and Reinisch. (2008).This is in contrast to the work of Bhuyan and Borah. (2007), which compared the TEC measured using GPS satellites along a chain of Indian stations with that predicted by the IRI-2001 for the low solar activity year 2004 during solar cycle 23. It was found that IRI

overestimated the TEC over Delhi (MLAT 18^0 N), a location near the northern edge of the EIA. Bhuyan and Hazarika. (2013) also compared the GPS derived TEC and the IRI model 2012 and found that during the low activity period of 2009–2010, the IRI underestimates the TEC in about all months and at all local times except in the months of October, 2009 with a near systematic difference of ~10 TECU between the measured and predicted TEC in the summer and winter solstice. In the equinoxes, however, the deviation of the estimated TEC gradually reduces and during the daytime peak hours, the two data sets almost become equal, which is in agreement with the present work. In the moderate solar activity year 2010–2011, IRI estimates TEC better and in certain months e.g. in July 2011 matches observed TEC. Rabiu *et al.*, (2014). Compared the IRI and the NeQuick model with the derived TEC in Nigeria and found that the IRI and NeQuick modelled values follow the diurnal and seasonal variation patterns of the observed values of VTEC and generally the models underestimated the derived TEC except during the decsols.

4.4. ROOT MEAN SQUARE ERROR ANALYSIS

Figures 4.23 to 4.30 show the differences between the VTEC and the IRI model for the seasonal classifications for the two stations

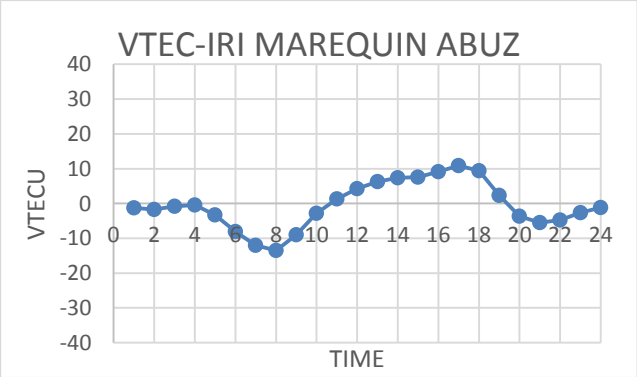

Figure 4.23 VTEC–IRI

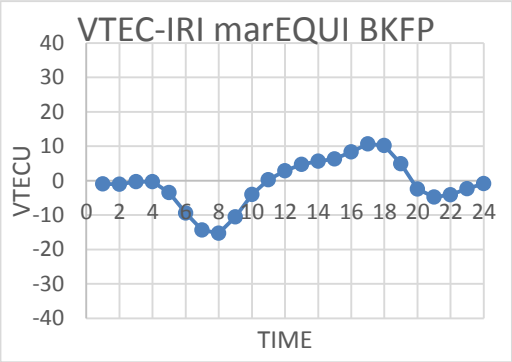

Figure 4.24 VTEC–IRI

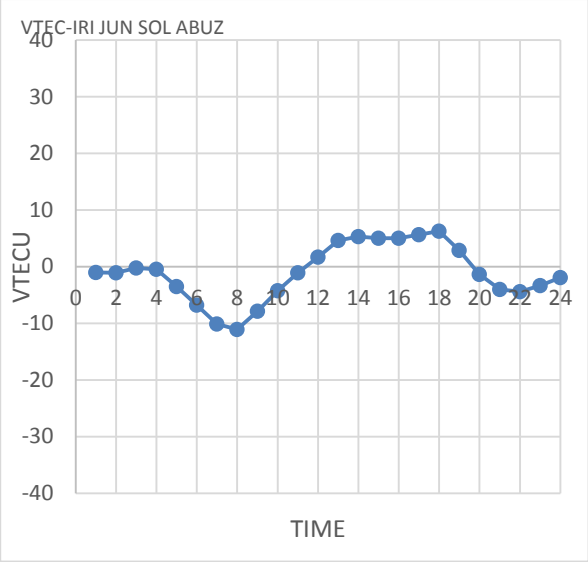

Figure 4.25 VTEC–IRI

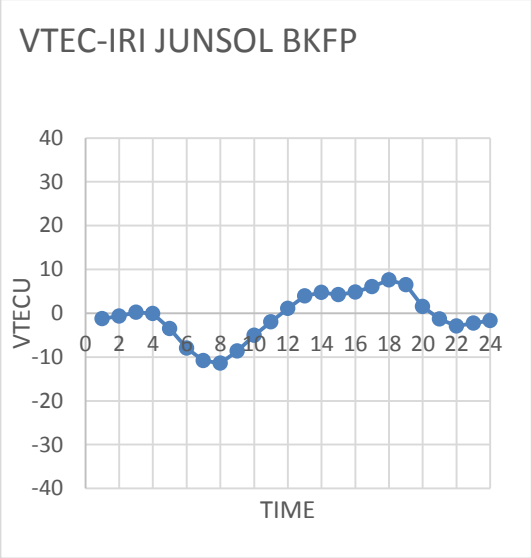

Figure 4.26 VTEC–IRI

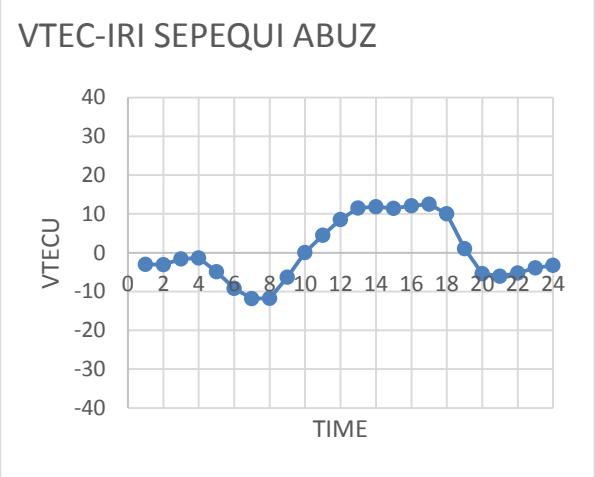

Figure 4.27 VTEC–IRI

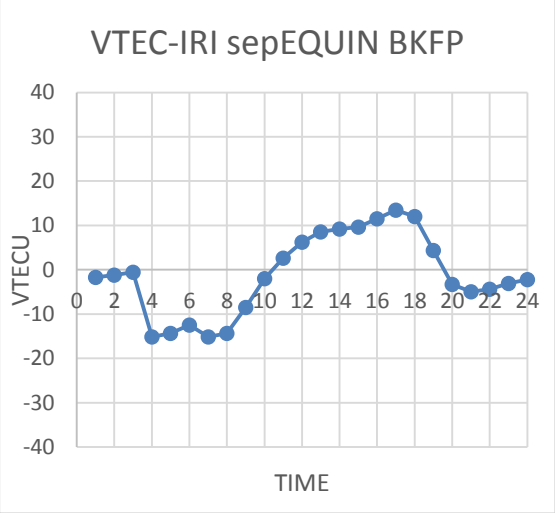

Figure 4.28 VTEC–IRI

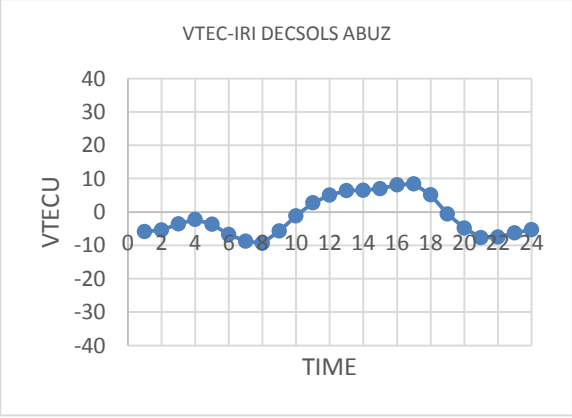

Figure 4.29 VTEC–IRI

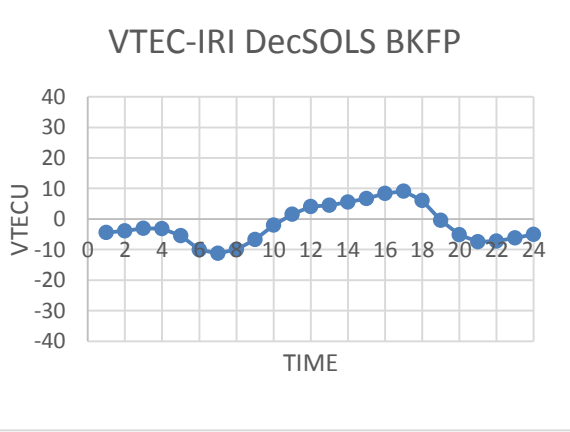

Figure 4.30 VTEC–IRI

4.4.1. DISCUSSION

For this work, the plots showed that the prediction are relatively good during the night and the forecasting during daytime is worst, most especially during equinoctial month (10TECU to 12 TECU) the difference between experimental VTEC and modeled VTEC shown in Figures 4.23-4.30 shows that in the night time between the hours of 24:00 to 4:00 LT the model almost matches the GPS derived TEC in June solstice, march equinox and September equinox compared to December solstice in both the two stations with a gradual decreased reaching to a minimum peak at about 8:00 LT which is the highest overestimation by the model for both the two station and all the seasons, also in September equinox the model almost matches the GPS derived TEC between the hours of 24:00 to 3:00 LT and a gradual decreased in the negative difference with a two peaks between the hours of 4:00 and 8:00LT that is to say two highest overestimation by the model is observed in September equinox.

There is a gradual increased reaching to a highest positive value with a peak occurred mostly around 17:00-18:00 LT which is the highest underestimation by the model followed by a gradual decreased .A second peak in the negative difference in TEC occurs around 20:00-21:00 LT, there is an over estimation by the model between this hours this means that during the day hour there is actually an under estimation by the model, the over estimation which occurs during the night between 4:00 to 8:00LT and 20:00-21:00LT varies from month to month and season to seasons. The highest TEC over estimation is observed in the sepequinox with RMSE average of 9TECU followed by March equinox and the lowest RMSE average is observed in the June solstice with a RMSE of 5TECU. The RMSE average differences between the solstice seasons is ±1.07 and is ±2.13during the equinoxes this shows that the model predict well during solstice months. The over estimation by VTEC may be attributed to the equatorial ion effect (Leong *et al., 2014)*, solar cycle number 24 and to the plasmaspheric content (Rabiu, *et al.*, 2012). The experimental GPS-VTEC was calculated along the propagation path of a satellite-

emitted signal from an altitude of 20,200 km over the Earth to the GPS receivers; however, the upper boundary for the predicted VTEC is 2000 km, this may be one reason for the observed difference in the measured and modeled values. As pointed out by other researchers (Luhr and Xiong, 2010; Sethi, *et al.*, 2011), the prediction which primarily occur during the day time hours could be due to the fact that the model is strongly underestimating the equatorial ion fountain effects' lower variability (Olawendo, *et al.*, 2012). Also, the discrepancies observed may result from an inaccurate correction factor for the IRI model (Bilitza, 2004; Bilitza and Reinisch, 2008) and an inaccurate Epstein layer with a height dependent thickness (i.e. scale height) parameter (Rabiu, *et al.*, 2012).

The RMSE analysis for the seasonal classification was done for the two stations:

Table 4.1: RMSE for the two stations compared with the IRI Model

	MARCHEQUINOX	JUNSOLS	SEPEQUI	DECSOLS
BKFP	6.88	5.26	9.01	6.33
ABUZ	6.52	5.00	7.82	6.03

4.5. STATISTICAL ANALYSIS

4.5.1. Introduction

A time series is a set of observations obtained by measuring a single variable regularly over time. Time series forecasting is the use of a model to predict future events based on known past events. In time series, the past provides a model for the future, time series analysis can make use of these predictor fields to increase the accuracy of the predictions. A crucial feature of the IBM SPSS Forecasting module is the *Expert Modeller*. Rather than defining the parameters and settings of time series models manually, the *Expert Modeller* automatically identifies and estimates the best-fitting ARIMA or exponential smoothing model for one or more dependent variable series. Although users can specify a custom ARIMA or exponential

smoothing model manually, *Expert Modeller* eliminates a great deal of the trial and error associated with doing so.

All the data used in both the two station were further analyzed using SPSS Time series analysis with a date format of Hour and day. The details of the output are shown in the tables below.

Table 4.2a. ARIMA Model Description IRI ABUZ

			Model Type
Model ID	IRIABUZ	Model_1	ARIMA(4,0,6)(0,1,0)

Table 4.2b. Model Statistics IRI ABUZ

Model	Number of Predictors	Model Fit statistics			Ljung-Box Q(18)			Number of Outliers
		Stationary R-squared	R-squared	RMSE	Statistics	DF	Sig.	
IRIABUZ-Model_1	0	.846	.992572	1.035	1481.993	12	.000	0

Table 4.2c. ARIMA Model Parameters IRI ABUZ

				Estimate	SE	t	Sig.
IRIABUZ-Model_1	IRIABUZ	AR	Lag 2	.397	.014	27.828	.000
			Lag 4	-.174	.013	-13.331	.000
		MA	Lag 1	-1.667	.009	-192.425	.000
			Lag 2	-1.182	.006	-183.498	.000
			Lag 4	.458	.005	96.320	.000
			Lag 6	-.153	.005	-29.041	.000
		Seasonal Difference		1			

Table 4.3a. ARIMA Model Description IRI ABUZ

			Model Type
Model ID	VTECABUZ	Model_1	ARIMA(1,0,10)(1,1,1)

Table 4.3b. ARIMA Model Statistics VTECABUZ

Model	Number of Predictors	Model Fit statistics			Ljung-Box Q(18)			Number of Outliers
		Stationary R-squared	R-squared	RMSE	Statistics	DF	Sig.	
VTECABUZ-Model_1	0	.748	.976	2.601	65.156	12	.000	0

4.3c. ARIMA Model Parameters VTECABUZ

				Estimate	SE	T	Sig.
VTECABUZ-Model_1	VTECABUZ	AR	Lag 1	.875	.007	122.106	.000
			Lag 2	.097	.013	7.419	.000
		MA	Lag 3	.073	.012	5.819	.000
			Lag 10	.045	.011	4.042	.000
		AR, Seasonal	Lag 1	.069	.013	5.543	.000
		Seasonal Difference		1			
		MA, Seasonal	Lag 1	.881	.006	140.782	.000

4.4a. Model Description IRIBKFP

			Model Type
Model ID	IRIBKFP	Model_1	ARIMA(4,0,8)(0,1,0)

4.4b. Model Statistics IRIBKFP

Model	Number of Predictors	Model Fit statistics			Ljung-Box Q(18)			Number of Outliers
		Stationary R-squared	R-squared	RMSE	Statistics	DF	Sig.	
IRIBKFP-Model_1	0	.911	.999	.388	1382.565	8	.000	0

4.4c. RIMA Model Parameters IRIBKFP

			Estimate	SE	t	Sig.
IRIBKFP-Model_1	IRIBKFP	Lag 3	-.901	.002	-512.632	.000
		Lag 4	-.157	.002	-89.310	.000
		Lag 1	-1.887	.009	-206.426	.000
		Lag 2	-1.990	.019	-103.499	.000
		Lag 3	-2.312	.023	-100.506	.000
		Lag 4	-2.693	.022	-120.176	.000
		Lag 5	-2.374	.023	-105.063	.000
		Lag 6	-1.588	.023	-68.160	.000
		Lag 7	-1.003	.019	-51.884	.000
		Lag 8	-.505	.009	-55.438	.000
		Seasonal Difference	1			

4.5a Model Description VTECBKFP

			Model Type
Model ID	VTECBKFP	Model_1	ARIMA(2,0,10)(0,1,1)

4.5b. Model Statistics VTECBKFP

Model	Number of Predictors	Model Fit statistics			Ljung-Box Q(18)			Number of Outliers
		Stationary R-squared	R-squared	RMSE	Statistics	DF	Sig.	
VTECBKFP-Model_1	0	.769	.976	2.592	38.870	12	.000	0

4.5c. ARIMA Model Parameters VTECBKFP

				Estimate	SE	t	Sig.
VTECBKFP-Model_1	VTECBKFP	AR	Lag 1	1.312	.070	18.759	.000
			Lag 2	-.428	.060	-7.117	.000
		MA	Lag 1	.352	.073	4.827	.000
			Lag 6	-.036	.012	-2.952	.003
			Lag 10	.044	.011	4.044	.000
		Seasonal Difference		1			
		MA, Seasonal	Lag 1	.769	.007	110.033	.000

.

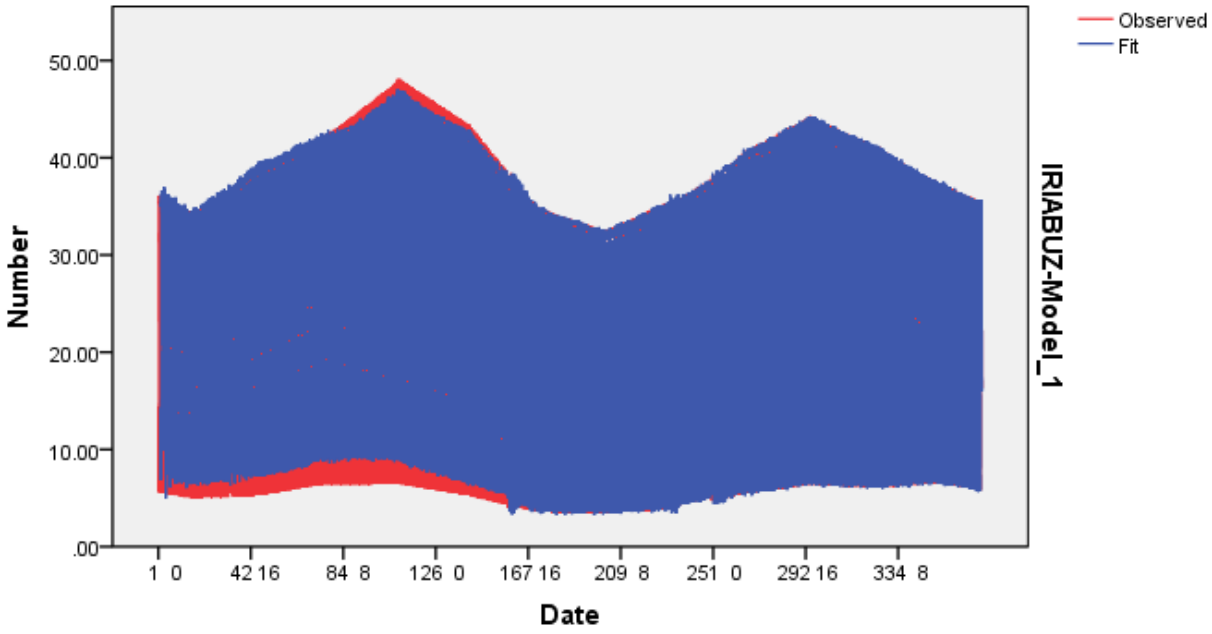

Figure 4.31 IRI observed and predicted (fit) for ABUZ station

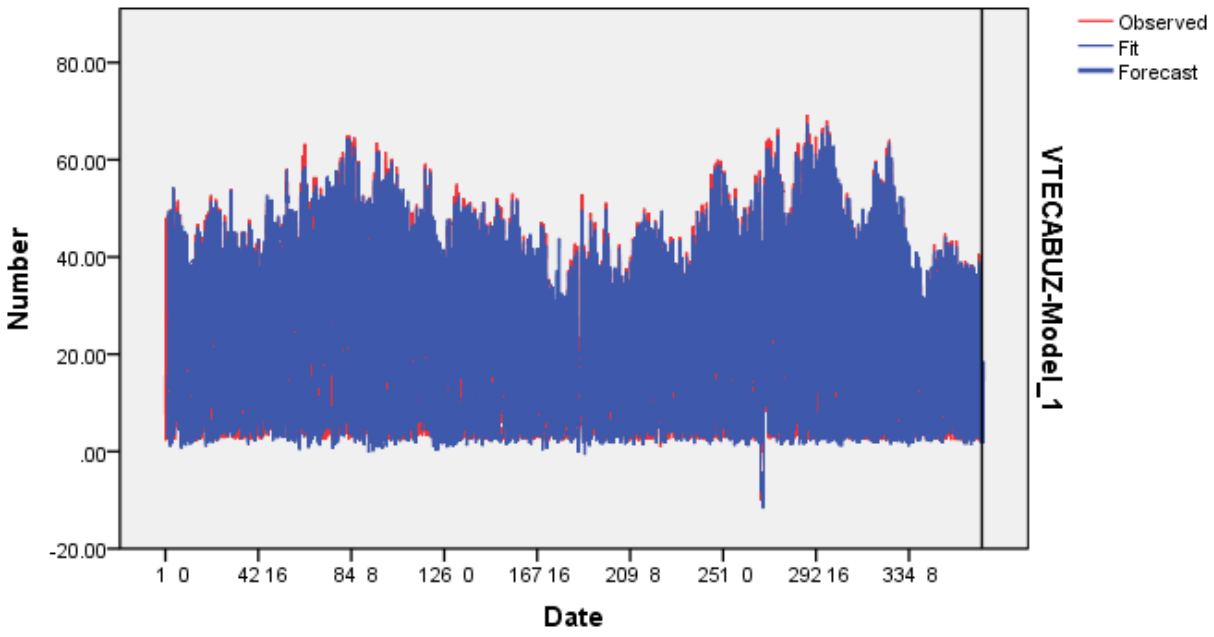

Figure 4.32 GPS VTEC observed and predicted (fit) for ABUZ GPS station.

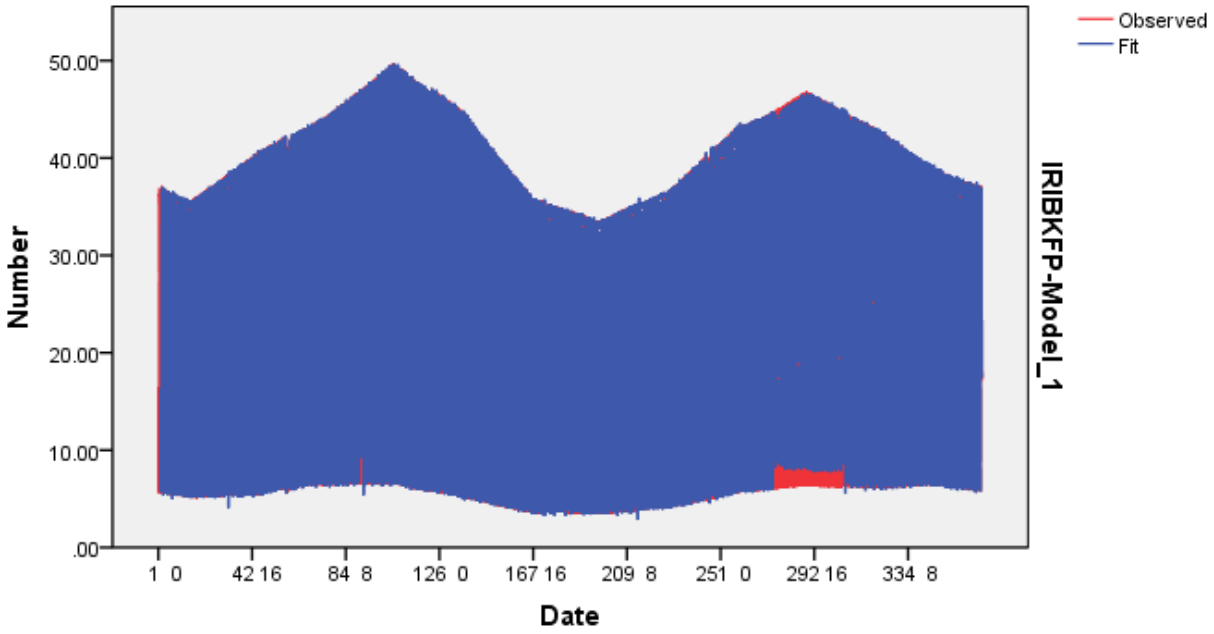

Figure 4.33. IRI observed and predicted (fit) for BKFP station

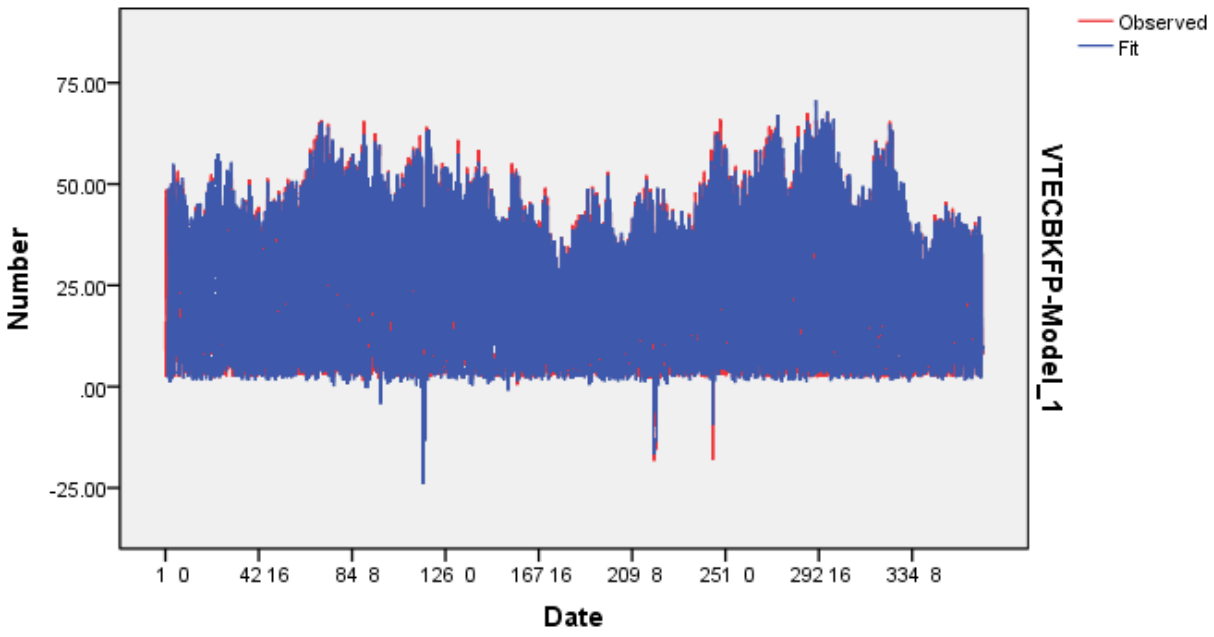

Figure 4.34. GPS VTEC observed and predicted (fit) for BKFP GPS station

4.5.2. DISCUSSION

In interpreting the tables above we are concerned with the columns headed ".Sig", stationary R square and R square. These columns give the p-values for the significance test as our result from the model parameters the p value is less than 0.05 significance level, this result is considered significant. The conclusion from the Ljung–Box test is similar for both the two stations and also for both the IRI and GPS derived TEC and also the tables give a stationary R square of 84.6%, 74.8%, 91.1% and 76.9% and R square of 99.2%, 97.6%, 99.9% and 97.6 for IRIABUZ, VTECABUZ, IRIBKFP and VTECBKFP respectively. It was found that for all the model statistics and the model parameters The P-value which is less than 0.05 indicates that there is an evidence that the residuals are dependent and the model is good so also the parameters of a model are accepted as significant since the estimated value of the parameter is twice the standard error of this estimate or more. The conclusion from the Ljung–Box test is similar. This further confirms that the ARIMA model type chose by expert modeler is adequate. If the P-value was below about 0.05, there would be some cause for concern: from the above tables it was found that "there was evidence of an association between IRI and

VTEC. The comparison between the modeled value and observables are shown in Fig. 4.31, 4.32, 4.33 and 4.34 for both the IRI and VTEC and in both the two stations. The modeled result matches the observables very Well which also shows the goodness of the time series model. The statistical error clearly exhibits a normal distribution. We therefore conclude that the time series model can accurately represent the daily averaged TEC. The RMS between observed and modeled daily averaged TEC for the two stations are shown in the tables above which is better for the IRI model than for the VTEC. In the deterministic picture, irregularity can be autonomously generated by the nonlinearity of the intrinsic dynamics of the system, which may be a possible reason for chaoticity of ionosphere even at quiet conditions Shuhui et al (2013). It is known that ionosphere plasma density is determined mainly by solar photoionization, neutral composition, winds, plasma diffusion, and electrodynamics during magnetic quiet periods. The influence of different causative mechanisms and their nonlinear interdependencies gives sufficient reason for the complexity and nonlinear aspects of ionospheric parameters like TEC (Unnikrishan and Ravindram, 2010). It is known that E×B drift brings plasma from low to high altitudes during day time and from high to low altitudes (down- ward) during night, the electron density peaks are observed in the noon and evening (Pavlov etal.,2004). The local time variations of the neutral wind, electric fields, and production recombination rates produce inherent irregularities leading to chaotic variations, even at quiet time ionosphere. The turbulent upwelling of ionosphere, effects of sub storms and major storms on the equatorial ionosphere/thermosphere system, etc. can make the situation more and more complex.

Numerous researchers have utilized linear time series models to quantitatively determine the impact of different factors on ionospheric TEC climatological variations. Forbes *et al*. (2000) adopted multiple linear regression analysis and considered annual and semiannual terms as well as the solar F10.7 index and its 81-day mean value as influencing factors to construct an

empirical model. The constructed model is useful in studying the effects of solar activity and season variability on F-region peak plasma density. Yu *et al*. (2009) studied the linear model of global ionospheric TEC standard deviation covariance with the F10.7 index, geomagnetic Ap index, and periodic change. Yu et al.'s (2009) results proved that solar activity and season variations are dominant factors.

CHAPTER FIVE

SUMMARY, CONCLUSION AND RECOMMENDATIONS

5.1. SUMMARY.

The GPS derived TEC data over two different equatorial stations in Nigeria are used to study the diurnal and seasonal variation of TEC and the result are compared with the IRI model 2012. The diurnal behavior of TEC shows a night time maintenance of ionization the day time ionization is maximum compared with the night time over the two stations and the density of TEC is higher in equinoctial months and lower during the summer months which is a winter anomaly, a comparative study has been made between the IRI 2012 model and the derived TEC which shows that in all the plots of the comparison the VTEC overestimated the IRI model in all the months and in both the two stations and in all the seasonal classifications , a RMSE analysis has been employed to quantify the performance of the model, the GPS TEC shows good agreement mostly during the night time and an underestimation by the model during the day time between the hours of 1300LT - 1700LT and an over estimation during the sunrise and sunset period in all the months and seasons. The model predict well during the solstice months with a lowest RMSE in solstice months than the equinoxes.

5.2. CONCLUSION.

The research work present the analysis of the variation of total electron content over two equatorial stations in northern Nigeria, using measurement of slant total electron content from the GPS receiver .The mean diurnal monthly, and seasonal variations in TEC during the moderate solar activity phase was discussed .The main results of this study are as follows:

- Estimated TEC values over BKFP during a moderate solar activity period have very similar values to those measured over ABUZ
- The value of VTEC shows seasonal variation with a maximum occurrence in Equinox months and minimum in winter and summer this may be due to EEJ strength, which

maximizes in Equinox month and minimizes in summer and winter and also is due to vertical E×V which is upward in winter and down ward in summer

- Seasonal variations in day time TEC show a semiannual periodicity, with maxima in equinoxes and minima in solstices with March equinox having the maximum peak in TEC and June solstice the minimum.
- The diurnal averages for various months show a higher value in BKFP than ABUZ The result of the various month and seasonal result have been subjected to RMSE analysis to quantify the performance of the IRI model 2012 for the year 2012
- The trends of the IRI VTEC calculated follows the same pattern, the model underestimated during day time and overestimated mostly during night hours so also during the sunrise and the sunset period.
- The seasonal variation in day time TEC shows a maxima in equinox and minima in solstices with March equinox having the highest peak in TEC and June solstice experience the lowest intensity of VTEC
- The data for the two stations; Birnin Kebbi and Zaria show almost the same monthly and seasonal VTEC variation patterns. Their RMSE are almost the same except for the September Equinox for Birnin Kebbi, which shows a higher value. The IRI Model generally under estimate the observed TEC during the noon time and overestimate mostly during the sunrise and sunset. As explained earlier this could be due the fact that the measured GPS-VTEC was calculated along the propagation path of a satellite-emitted signal from an altitude of 20,200 km over the Earth to the GPS receivers; while the upper boundary for the predicted IRI VTEC is 2000 km.

5.3. RECOMMENDATIONS

There is a need to have more GPS stations in Nigeria more especially the equatorial region because of the effect of ionosphere in that region

Further study is needed of the circumstances leading to potentially serious errors at times of severe geomagnetic disturbance when localized gradients associated are with storm enhanced density structures.

There is a need to improve the ionospheric models and improving the mapping of structures in the regional ionosphere, further work is needed in key areas, particularly in relation to the reliability of both measurements and resultant products at times of steep gradients in the low-latitude ionosphere during the onset phase of geomagnetic storms. In addition, the ability of models to replicate conditions in the vicinity of the main trough also needs investigation.

There is a need for Nigeria space research organization, Nigerian air force and the Nigeria airport authority to jointly launch a project similar to the wide area augmentation system of united states of America in order to study and monitor the temporal and spatial behaviour of ionosphere using the continues measurement of TEC and scintillation data.

Further study is needed for continues measurement of TEC from all the longitude and latitude zones of Nigeria in order to monitor the unique behavior of TEC in the entire country.

Also for further study there is a need to use time series analysis to analyses and validated both the GPS derived TEC and the IRI model and to create a time series model for both the IRI and VTEC.

5.4. REFERENCES

Abdullah, M, Zain. A.F.M.,Ho Y.H. and Abdullah s. (2009) TEC and Scintillation Study of Equatorial Ionosphere: A Month Campaign over Sipitang and Parit Raja Stations, *Malaysia American J. of Engineering and Applied Sciences 2 (1): 44-49, ISSN 1941 7020.*

Ackrroyd, N., Lorimer, R. A GPS User's Guide. Lloyd's of London Press, 1990. P 120

Adebiyi. S. J. Odeyemi. O. O, Adimula. I. A, Oladipo. O. A, Ikubanni. S. O, Adebesin. B. O, Joshua. B. W. (2014) GPS derived TEC and foF2 variability at an equatorial station and the Performance of IRI-model. *Advances in Space Research* 54. 565–575.

Adewale, A.O., Oyeyemi, E.O., Cilliers, P.J., McKinnell, L.A., Adeloye, A.B., (2012). Low Solar activity variability and IRI 2007 predictability of equatorial Africa GPS TEC. *Adv. Space Res*. 49, 316–326.

Adohi, J.-P., Vila, P.M., Amory-Mazaudier, C., Petitdidier, M., (2008). Equinox transition at the magnetic equator in Africa: analysis of ESF ionograms. *Ann. Geophys*. 26 (7), 1777-1792.

Alothman. A.O., Alsubaie. M.A., Ayhan. M.E. (2011) Short term variations of total electron Content (TEC) fitting to a regional GPS network over the Kingdom of Saudi Arabia (KSA), *Advances in Space Research* 48 (2011) 842–849.

Bagiya, M.S., Joshi, H.P., Iyer, K.N., Aggarwal, M., Ravindran, S., Pathan, B.M., (2009). TEC Variations during low solar activity period (2005–2007) near the equatorial ionospheric Anomaly crest region in India. *Ann. Geophys*. 27, 1047–1057.

Balan, N., Batista, I.S., Abdu, M.A., Bailey, G.J., Watanabe, S., MacDougall, J., Sobral, J.H.A., (2000). Variability of additional layer in the equatorial ionosphere over Fortaleza. *J. Geophys. Res.* 105, 10603–10613.

Belehaki, Reinhart Leitinger, Sandro M. Radicella, Cathryn N. Mitchell and Paul S.J. Spencer (2004) Total electron content: A key parameter in Propagation: Measurement and use in ionospheric imaging. *Annals of Geophysics, Supplement to vol*. 47, n. 2/3, 200.

Bhuyan, P.K. and Borah, R.R., (2007). TEC derived from GPS network in India and comparison With the IRI. *Advances in Space Research*. 39, 830–840.

Bhuyan, P.K., Hazarika, R., (2013). GPS TEC near the crest of the EIA at 95^0 E during the ascending half of solar cycle 24 and comparison with IRI simulations. *Adv. Space Res.* 52, 1247–1260.

Bhuyan, P.K., Chamua, M. (2002). Electron density measurements in the topside F-region and its comparison with the IRI in the 75_E longitude sector. *J. Atmos. Sol. Terr. Phys.* 64, 55–64.

Bilitza, D. (2014). The International Reference Ionosphere – Status 2013 *J. Adv. Space Res.* (2014),

Bilitza, D., Reinisch, B.W., (2008). International reference ionosphere 2007: Improvements and new parameters. *J Adv. Space Res.* 42, 599–609.

Bolaji. O.S., J.O.Adeniyi , I.A.Adimula , S.M.Radicella , P.H.Doherty,(2013), Total electron Content and magnetic field intensity over Ilorin, Nigeria, *Journal of Atmospheric and Solar-Terrestrial Physics* 98 (2013) 1–11.

Bolaji, O. S, Adeniyi J.O, Radicella. S. M, and Doherty. P.H (2012) Variability of total Electron content over an equatorial West African station during low solar activity Radio Science, Vol. 47, and Rs1001.

Chauhan.V and Singh, O.P., (2010). A morphological study of GPS–TEC data at Agra and their comparison with the IRI model. *Journal of Advances in Space Research: The Official Journal of the Committee on Space Research (COSPAR)* 46, 280–290.

Chakraborty S.K, and .Hajra R. (2010) Variability of total electron content near the crest of the equatorial anomaly during moderate geomagnetic storms. *Journal of Atmospheric and Solar-Terrestrial Physics* 72, 900–911.

Chin-Chun Wu, K. Liou, Shao-Ju Shan, Tseng C.-L. (2006), Variation of ionospheric total Electron content in Taiwan region of the equatorial anomaly from 1994 to 2003, *Advances in Space Research* 41, (2008). 611–616.

Coco, D. GPS satellites of opportunity for ionospheric monitoring. GPS World, 47, (1991).

Da Costa, A.M., Boas, J.W.V., da Fonseca Jr., E.S., 2004. GPS total electron content Measurements at low latitudes in Brazil for low solar activity. *Journal of Geophysical Inter National* 43 (1), 129–137.

Davies, K. (1980) recent progress in satellite radio beacon studies with particular emphasis On the ATS-6 Radio beacon experiment, *Journal of Space Sci. Rev.*, 25, 357–430,

Davies, K. Ionospheric radio. Peter Peregrinus Ltd., London, (1990). ISBN 0-86341-186-X.

De Toma, G.; White, O.R.; Knapp, B.G.; Rottman, G.J., and Woods, T.N. (1997) Mg II core -to-wing Index: Comparison of SBUV2 and SOLSTICE time series. *Journal of Geophysic Research*, 102:2597–2610.

De Toma, G.; White, O.R.; Chapman, G.A.; Walton, S.R.; Preminger, D.G.; Cookson,

A.M. And Harvey, K.L.(2001) Differences in the Sun's Radiative Output in Cycles 22 and 23. *The Astrophysical Journal Letters,* 549:L131–L134.

Ezquer, R., Brunini, C., Mosert, M., meza, A., Del, R., Oviedo, V., Kiorcheff, E., Radicella, S., (2004). GPS-VTEC measurements and IRI predictions in the South America Sector. *Advances in Space Research: The Official Journal of the Committee on Space Research* (COSPAR) 34 (9), 2035–2043

Fayose.R.S, Rabiu B, Olakunle O & Keith G. (2012) Variation of Total Electron Content [TEC] and Their Effect on GNSS over Akure, Vol. 4, No. 2; 2012.

Forbes, J.M., Palo, S.E., Zhang, X.(2000) Variability of the ionosphere. *J. Atmos. Solar-Terr. Phys*. 62, 685–693.

Hoffmann-Wellenhof, B., H. Lichtenegger, and J. Collins, (1994) Global Positioning System: Theory And Practice, 3rd ed., New York: Springer-Verlag..

Hoque, M. M and N. Jakowski (2010). Higher order ionospheric propagation effects on GPS radio occultation signals. *Advances in Space Research,* 2010. 46(2): pp. 162-173.

Huang Y N. (1978). Solar cycle variation in the total electron content at Sagamore Hill. *J. Atmos. Terr. Phys.* **40,** 733-739.

Iyer, K.N., Joshi, H.P., Jivrajani, R.D., Aravindakshan, P. (1996). Comparative study of TEC near The crest of the equatorial anomaly with IRI model for solar minimum to solar maximum. *J. Adv. Space Res.* 18 (6), 233– 236.

Kelley, M.C. (1989). The Earth's Ionosphere: Plasma Physics and Electrodynamics (Academic Press, San Diego, 1989).

Kersley, L., D. Malan, S.E. Pryse and Lj.R.Cander (2004): Further investigations on the Verification of TEC measurements by different techniques, in Proceedings of the 3rd COST 271 Workshop, 23-27 September 2003, Spetses, Greece. *ANNALS OF GEOPHYSICS, SUPPLEMENT TO VOL*. 47, N. 2/3, 2004

Kersley, L., D. Malan, S.E. Pryse, Lj.R. Cander and R.A. Bamford (2002): Progress towards Verification and validation of TEC observations over Europe, in Proceedings of the COST271 Workshop, 2-4 October 2002, Faro, Portugal.

Klobuchar, J.A. and J.M. Kunches, (2000). Eye on the Ionosphere: The spatial variability of ionospheric range delay. GPS Solution, 3: 70-74.

Klobuchar, J. A. (1996), Ionospheric effects on GPS, in Global Positioning System: Theory And Applications, Progress Astronaut and Aeronaut. Ser., vol. 164.

Kumar. S, and Singh A.K. (2009), Variation of ionospheric total electron content in Indian low latitude region of the equatorial anomaly during May 2007–April 2008 *Www.sciencedirect.com. Advances in Space Research*. 43, (2009). 1555–1562.

Langley, R. B., (1990) .Why is the GPS Signal So Complex? GPS World, Vol. 1, No. 3, May/June, pp. 56.59.

Le Huijun , Libo Liu, Jann-Yeng Liu , Biqiang Zhao, Yiding Chen , Weixing Wana;(2013) The ionospheric anomalies prior to the M9.0 Tohoku-Oki earthquake. *Journal of Asian Earth Sciences* 62 (2013) 476–484

Legrand, Simon, 1989. Solar cycle and geomagnetic activity: a review for geophysicists. Part I. The contributions to geomagnetic activity of shock waves and of the solar wind. *Ann. Geophys.* 7 (6), 565–578.

Leonard kersley, Daniel Mala, S. Eleri Pryse, Ijiljana R. Cander, Ruth A. Bamfor , Anna S.K. Leong, T.A. Musa, K. Omar, M.D. Subari, N.B. Pathy, M.F. Asillam (2014)Assessment of ionosphere models at Banting: Performance of IRI-2007, IRI -2012 and NeQuick 2 models during the ascending phase of Solar Cycle 24 *Retrived. www.sciencedirect.com.*

Liu, J.-Y., Chen, C.-H., Lin, C.-H., Tsai, H.-F., Chen, C.-H., Kamogawa, M., (2011b). Ionospheric disturbances triggered by the 11 March 2011 M9.0 Tohoku earthquake. *Journal of Geophysical Research* 116, A06319.

Luhr, H., Xiong, C., (2010). IRI-2007 model overestimates electron density during the 23/24 Solar minimum. *Geophysical Research Letters*, L23101.

Mannucci, A.J., B. Iijima, L. Sparks, P. Xiaoqing, B. Wilson and U. Lindqwister, (1999). Assessment of global TEC mapping using a three-dimensional electron density model. *Journal of Atmospheric and Solar-Terrestrial Phy.*, 61: 1227-1236.

Mannucci, A., Wilson, B., Yuan, D., Ho, C., Lindqwister, U., & Runge, T. (1998). A global Mapping technique for GPS derived ionospheric total electron content measurements. *J. Radio Sci.*, 33(3), 565-582.

Mannucci, A.J., Wilson, B.D., Edwards, C.D., (1993). A new method for monitoring the earth's Ionosphere total electron content using the GPS global network, Proceedings GPS-93. Institute of Navigation, pp. 1323–1332.

Maruyama, T., Ma, G., Nakamara, M., (2004). Signature of TEC storm on 6 November 2001 derived from dense GPS receiver network and ionosonde chain over Japan. *J. Geophys. Res.* 109, A10302.

Matsushita, S., Campbell, W.H., (1967).Physics of Geomagnetic Phenomena, vols.1–2. Academic Press, New York and London.

Mekaoui, S. and Dewitte, S. (2007) Total Solar Irradiance Measurement and Modelling during Cycle 23. *Solar Physics*, 247(1):203–216.

Memarzadeh, Y. Ionospheric modeling for precise GNSS applications. PhD thesis, Technische Universiteit Delft, Netherlands, 2009.

Najman,P and Kos,T (2014) Performance Analysis of Empirical Ionosphere Models By Comparison with CODE Vertical TEC Maps

Ngwira. C. M, Lee-Anne M, Pierre J. C, Endawoke Y. (2012) An investigation of ionospheric disturbances over South Africa during the magnetic storm on 15 May 2005, *Retrieved www.sciencedirect.com Advances in Space Research* 49 (2012) 327 –335.

Olapido, O.A., Adeniyi, J.O., Radicella, S.M., Obrou, O.K., (2008). Variability of equatorial ionospheric density at fixed heights below the F2 peak. *J. Atmos. Terr. Phys.* 70, 1056 –1065.

Olwendo, O.J., P.Baki, C.Mito, P.Doherty (2012). Characterization of ionospheric GPS Total Electron Content (GPS–TEC) in low latitude zone over the Kenyan region during a Very low solar activity phase. *Journal of Atmospheric and Solar-Terrestrial Physics* 84-85 (2012) 52–61 a.

Ouattara, F., Gnabahou, A., Amory-Mazaudier, C.,(2012). Seasonal, diurnal and solar-cycle Variations of electron density at two West Africa equatorial ionization anomaly stations. *Int. J. Geophys.* 2012, 1–9.

Pavlov, A.V., Fukao, S., Kawamura, S., (2004). Comparison of the measured and modeled electron densities, and electron and ion temperatures in the low-latitude ionosphere during 19–21 March 1988. *Annales Geophysicae* 22, 2747–2763.

Prasad S.N.V.S., P.V.S. Rama Rao, D.S.V.V.D. Prasad, K. Venkatesh, K. Niranjan (2011) on the Variabilities of the Total Electron Content (TEC) over the Indian low latitude sector. *Advances in Space Research* 49 (2012) 898–913

Rabiu. B. (2011). National space Research and Development Abuja The equatorial Ionosphere a tutorial 2011.

Rabiu, A.B, A.O. Adewale, R.B. Abdulrahim, E.O. Oyeyemi (2014) TEC derived from some GPS stations in Nigeria and comparison with the IRI 2011 and NeQuick models. *Advances in Space Research* 53 (2014) 1290–1303.

Rama Rao, P.V.S., Gopi Krishna, S., Niranjan, K., & Prasad, S. V. V. D. (2006). Temporal and spatial variations in TEC using simultaneous measurements from the Indian network of receivers during the low solar activity period of 2004-2005. *Annales Geophysicae*, 24, 3279-3292.

Rama Rao, P.V.S., Gopi Krishna, S., Niranjan, K., Prasad, D.S.V.D., (2006). Temporal and spatial variation in TEC using simultaneous measurements from the Indian GPS network of receivers during low solar activity period of 2004–2005. *Annales Geophysicae* 24 (12), 3279–3292.

Rolland, L.M., Lognonné, P., Astafyeva, E., Kherani, E.A., Kobayashi, N., Mann, M . Munekane, H., (2011). The resonant response of the ionosphere imaged after the 2011 off The Pacific coast of Tohoku earthquake. Earth Planets. *Advance in Space* 63, 853 – 857.

Sharma S, Galav. P, Dashora N, Dabas R. S, Pandey R. (2012) Study of ionospheric TEC during space weather event of 24 August 2005 at two different longitudes. *Journal of Atmospheric and Solar-Terrestrial Physics* 75–76 (2012) 133–14

Shastri, S., Aggarwal, S., Sethi, N.K. (1996) Performance of IRI model prediction of F-region For Indian latitude. *Adv. Space Res*. 18 (6), 41–44.

Schunk, R.W., Nagy, A.F., (2009). Ionosphere, Physics, Plasma Physics and Chemistry. Cambridge University, Press.

Sethi, N.K., Dabas, R.S., Sarkar, S.K. (2011) Validation of IRI-2007 against TEC observations during low solar activity over Indian sector. *J. Atmos. Terr. Phys.* 73, 751–759.

Shimeis. A, Amory-Mazaudier. C, Fleury.R , Mahrous.A. M, Hassan. A. F. (2014), Transient Variations of vertical total electron content over some African stations from 2002 to 2012. j.asr.2014.07.038

Shuhui. L, Junhuan. P, Weichao. X, Kun. Q. (2013). Time series modeling and analysis of trends of daily averaged ionospheric total electron content. *Retrieved* *www.sciencedirect.com* *Advances in Space Research* 52 (2013) 801‑809

Shweta Mukherjee, Shivalika Sarkar, P.K. Purohit, A.K. Gwal (2010) Seasonal variation of Total electron content at crest of equatorial anomaly station during low solar activity Conditions. *Advances in Space Research* 46 (2010) 291–295.

Soicher H. and Gorman F. J (1985) Seasonal and day-to-day variability of total electron content at mid-latitudes near solar maximum. *Radio Sci.* 20, 383-387.

Sonnenberg, S.: Radio and Electronic Navigation, Chapter 7, Butterworth and Co, 6th Edition, 1988.

Tsugawa.T, Saito.A, Otsuka.Y, Nishioka.M, Maruyama.T, Kato.H, Nagatsuma.T, and Murata.K.T. (2011), Ionospheric disturbances detected by GPS total electron content observation after the 2011 off the Pacific coast of Tohoku Earthquake. *J. Earth Planets Space*, **63**, 875–879.

Unnikrishnan, K and Ravindran.S (2010). A study on chaotic behavior of equatorial/low latitudeionosphere over Indian sub-continent, using GPS-TEC time series. *Journal of Atmospheric and Solar-Terrestrial Physics* 72 (2010) 1080–1089

Walker G. O. and Ting S. D. (1972) Electron content and other related measurements for a low latitude station obtained at sunspot minimum by using a geostationary satellite. *J.Atmos. Terr. Phys.* 34, 283-294.

Wautelet Gilles (2013) Characterization of ionospheric irregularities and their influence on high-accuracy positioning with GPS over mid-latitudes Ph.D. *thesis Geomatics Unit, Department of Geography Faculty of Sciences, University of Liège Allée du Six Août,* 17 B-4000 Liège Belgium Tel. +32-4-366 57 44 E-mail. gilles.wautelet@ulg.ac.be

Wu, C.C., Fry, C.D., Liou, K., Tseng, C.L. (2004) Annual TEC variation in the equatorial Anomaly region during the solar minimum: September 1996–August 1997. *J. Atmos. Terr. Phys.* 66, 199–207.

Yashiro, S.; Gopalswamy, N.; Michalek, G.; Cyr, O.C. St.; Plunkett, S.P.; Rich, N.B., and Howard, R.A.(2004) A catalog of white light coronal mass ejections observed by the SOHO Spacecraft. *Journal of Geophysical Research*, 109 (A07105).

Yu, Y., Wan, W., Liu, L., (2009). A global ionospheric TEC perturbation index. Chin. *J. Geophys.* 52 (9), 2189‐2194 (in Chinese),